Contrails

FOREWORD

This report was prepared by Arthur D. Little, Inc., under Contract No. AF 33(616)-6816. This contract was initiated under Project No. 7381, "Materials Application", Task No 738101, "Exploratory Design and Prototype Development". It was administered under the direction of the Directorate of Materials and Processes, Deputy for Technology, Aeronautical Systems Division, with Lieutenant T. E. Lippart acting as project engineer.

This report covers the period from 15 January 1960 through 14 July 1961.

Approved for Public Release

Contrails

Approved for Public Release

Contrails

ABSTRACT

This program encompases an investigation of materials for vacuum insulation up to 4000°F. ADL-17, graphite fibers, thoria powder, and tantalum radiation shields were chosen as insulation components for long-term high-temperature tests on the basis of theoretical studies of both the mechanisms of heat transfer through evacuated insulation materials and preliminary experimental work. Thermal protection systems consisting of these materials were chemically and physically stable enough to be effective insulators for over 100 hours at temperatures of 3000°F and for several hours at 3500°F. Although we utilized only readily available materials, their insulating performance points to the potential effectiveness of improved materials.

PUBLICATION REVIEW

This report has been reviewed and is approved.

FOR THE COMMANDER:

W. G. RAMKE
Chief, Ceramics and Graphite Branch
Metals and Ceramics Laboratory
Directorate of Materials and Processes

Approved for Public Release

Contrails

TABLE OF CONTENTS

Approved for Public Release

Contrails

LIST OF TABLES

Approved for Public Release

Contrails

LIST OF FIGURES

Approved for Public Release

Contrails

I. INTRODUCTION

The need for attenuating heat flow at high temperatures has underlined the desirability of developing effective thermal insulating materials capable of operating under extreme conditions of temperature. A guide for the development of new insulating materials requires a basic understanding of the factors influencing the thermal properties of such materials. Various thermal properties have been investigated for more than 100 years; although the amount of literature on the subject is enormous, the mechanisms affecting heat flow and interactions between the parts of insulating materials are incompletely understood.

A thermal insulating material is a combination of gaseous and solid matter arranged in such proportions as to offer the most effective barrier to the passage of heat. Because single-component insulations are not sufficiently effective as insulators, a combination of materials that provide the maximum insulating effectiveness over the desired range of temperatures has to be developed. Such a thermal protection system can then be designed on the basis of insulating material and strength criteria to meet specific application requirements.

The use of vacuum insulation as an integral part of a thermal protection system is an attractive approach where maximum insulating effectiveness at high temperatures is required. Removing the gas phase from the insulation reduces the contribution to the over-all heat flow by the amount due to gas conduction, and the reactions of materials in an oxidizing atmosphere are reduced.

The aim of this program is to extend the demonstrated feasibility of vacuum insulations by an investigation of materials that can withstand temperatures up to 4000°F on the hot side. A thermal protection system operating in this temperature range can find many applications, as in a nuclear reactor, a rocket engine, or the protection of a hypersonic-speed vehicle from aerodynamic heating. Consider the example of a hypersonic vehicle as a typical application of a thermal protection system. The hypersonic boost-glide vehicle, unlike a missile, does not encounter its most severe heating problems only during the brief re-entry into the atmosphere. Depending upon the trajectory, aerodynamic heating during extended periods of flight through the upper atmosphere generates temperatures of several thousand degrees on the surfaces of this vehicle. To overcome the effect of aerodynamic heating under these nearly steady-stage conditions, an integrated system designed to protect various parts of a space vehicle has been developed (AF33(600)-37705).

Manuscript released by authors July 1961 for publication as an ASD Technical Documentary Report.

Approved for Public Release

Contrails

This type of integrated system has a weight advantage if applied to a "cooled structure" rather than to a "hot structure," which has many design problems associated with it. These problems are due to the difficulties of finding suitable materials of sufficiently high strength-to-weight ratios at elevated temperatures and to the associated nonstructural requirements for high-temperature electrical systems, hydraulic systems, bearings, and lubricants. A thermal protection system, which may take a number of structural forms, such as the double-wall construction, vacuum insulation construction, or a combination of the two, must combine maximum insulating effectiveness with the lowest possible weight. The advantage of a thermal protection system is that the insulating function and the load-carrying elements can be designed separately. The insulation can be designed to withstand the predicted heating conditions, and the load-carrying elements can be designed to withstand outside forces, such as aerodynamic loads, vibration, acceleration, thermal shock, and particle erosion. The insulating and load-carrying elements can then be combined to form the vehicle structure.

The outer wall surface of a thermal protection system may be either a heat-resistant material or a multi-element surface made up of small fabricated panels. The inner wall is formed by the outer shell of a conventional air frame structure using aluminum alloys. The protective layer of thermal insulation is enclosed between the two walls and may be either a permanently evacuated vacuum insulation or a self-evacuated insulation, relying on the low pressures existing at operating altitudes to evacuate the insulation.

The outer wall of the thermal protection system can be made to radiate heat by utilizing materials of high emissivity and by maintaining this outer wall at a relatively high temperature through efficient insulation. In this manner the external surfaces of the vehicle can dissipate most of the aerodynamic heat. However, even the remaining small portion of heat that may be conducted through the insulation may be more than the underlying primary structure can withstand. Therefore, it is essential that the insulating materials be capable of operating at a temperature gradient up to 4000°F on the hot side while remaining at an allowable low temperature on the side facing the primary structure; this temperature will depend upon the arrangement of suitable heat sinks and cooling media in the air frame. The system's insulating effectiveness is of the greatest importance in reducing the amount of coolant required for a particular mission, and it requires, therefore, that the function of the vacuum insulation and materials used in it be optimized for the desired operating conditions.

Approved for Public Release

Contrails

The choice of suitable insulating materials and of material combinations for high-temperature vacuum insulation has to be made on the basis of experimental measurement and analysis of the functional uses as well as the physical behavior of the materials. Recent developments of vacuum insulation for use at temperatures up to 2200°F have already shown the feasibility of the thermal protection system (Contract No. AF33(600)-40100 with AMC).

In order to extend the use of thermal protection systems to higher temperatures, the present investigation considered the following aspects: (1) development of criteria for efficient thermal insulations; (2) experimental and theoretical studies of the physical and chemical stability of several materials which promised to be efficient insulators; (3) experimental and theoretical investigation of their heat-transfer properties; and (4) investigation of the long-term behavior of the insulation systems at elevated temperatures.

Approved for Public Release

Contrails

II. MATERIALS SELECTION AND EVALUATION

A. CRITERIA FOR SELECTION

The satisfactory performance of a vacuum-insulation system at high temperatures depends upon the choice of suitable materials to withstand these temperatures and the time during which these materials are effective insulators. Desirable properties of an effective insulation material for use in a vacuum-insulation system are:

1. Low over-all density;
2. Particle size small enough to reduce gas conduction with a moderate vacuum;
3. Physical stability, indicated by a low vapor pressure at the operating temperatures and a softening point above the maximum operating temperature;
4. Chemical stability, indicated by lack of reactions with the container or other constituents of the insulation system;
5. Mechanical stability, indicated by lack of sintering and reasonable compressive strength;
6. Minimum contact area of particles with each other and with the container;
7. Ability to attenuate and scatter thermal radiation; and
8. Availability of component materials.

No single insulation component that fulfills all these requirements over the temperature range under consideration (100-4000°F) has been found; therefore, different materials were chosen for use in the warmer and cooler parts of the insulation system.

Approved for Public Release

Contrails

It is especially important that the insulation materials be selected on the basis of not only their insulating properties, but also their densities, since the product of thermal conductivity and density is what influences the potential application of the material in an airborne vehicle.

B. SELECTION OF MATERIALS

The selection of materials for evaluation as insulation components was based upon both theoretical considerations and experimental measurements of the physical and chemical properties of a large number of materials. The principal criteria considered were: (1) availability of materials; (2) physical properties; (3) chemical stability; (4) sintering; and (5) thermal conductivity. Potential insulation materials are discussed with respect to these criteria, and reasons for the final material selection are given.

1. Availability of Materials

Zirconia, graphite and carbon powder and fibers, titanium carbide, thoria, silicon carbide, magnesia, calcium oxide, aluminum nitride, boron, boron nitride, boron carbide, alumina, fibrous asbestos, and silicon nitride were all available as insulation material components. Carbon, graphite, and asbestos were available in fibrous form; other materials were available as powders of various particle sizes.

2. Physical Properties

Selected physical properties of several promising materials are presented in Table I. Theoretical densities of the solid material are given. The density of the powder materials is substantially lower than those given in Table I and depends on the particle size. The vapor pressures of several materials are presented in Figure 1 as functions of temperature. The values were calculated from thermodynamic data and measurements reported in the literature. (For details of calculation, see Second Semiannual Progress Report, January 10, 1961.)

For an insulation material to be stable at high temperatures in an evacuated system, its vapor pressure must be significantly lower than the pressure of the system. In order to reduce gas conduction to a low value at a temperature of 4000°F, a powder of 1-10 micron size requires a pressure of approximately 100-1000 microns Hg. (See Appendix A.) Pressure reduction is also necessary to reduce the possibility of chemical reactions. This criterion eliminates the use of AlN, SiC, B, BN, Al_2O_3, asbestos, B_4C, and Si_3N_4 in the hot zones of the insulation system. These components may, however, be used in the lower temperature zones.

Approved for Public Release

Contrails

TABLE I

SELECTED PHYSICAL PROPERTIES OF INSULATION MATERIALS

Compound	Melting Point (°F)	Density[a] (gm/cm^3)	Vapor Pressure at 4000°F (atm)	Reference
ZrO_2	4620	5.4	1.4×10^{-7}	(1)
C (Graphite)	6500	2.26	2.0×10^{-7}	(2)
TiC	5680	4.93	1.4×10^{-6}	(1, 2)
ThO_2	5520	10.03	3.7×10^{-6}	(1)
MgO	5070	3.65	2.4×10^{-5}	(1)
CaO	4680	3.37	2.73×10^{-5}	(1)
AlN	4350	3.05	1.3×10^{-1}	(1)
SiC	4710	3.22	1.7×10^{-1}	(1)
B	4170	2.34	3.1×10^{-1}	(2)
BN	5430	2.27	3.94×10^{-1}	(1)
Al_2O_3	3650	3.90	1 atm	(3)
Asbestos[b]	3000[c]	0.2-1.2[d]	1 atm	(3)
B_4C	4440	2.50	---	(3)
Si_3N_4[e]	3450	3.44	---	(3)

a. Theoretical density unless otherwise noted.
b. Composition given as: SiO_2-37-44%, MgO-39-44%, FeO-0-6%, H_2O-12-15%, CaO-0-5%, Fe_2O_3-0.1-5%, Al_2O_3-0.2-1.5%.
c. Approximate melting point of lowest melting constituent.
d. Various densities of materials are produced.
e. Sublimes at 1 atm pressure and 3450°F.

Approved for Public Release

Contrails

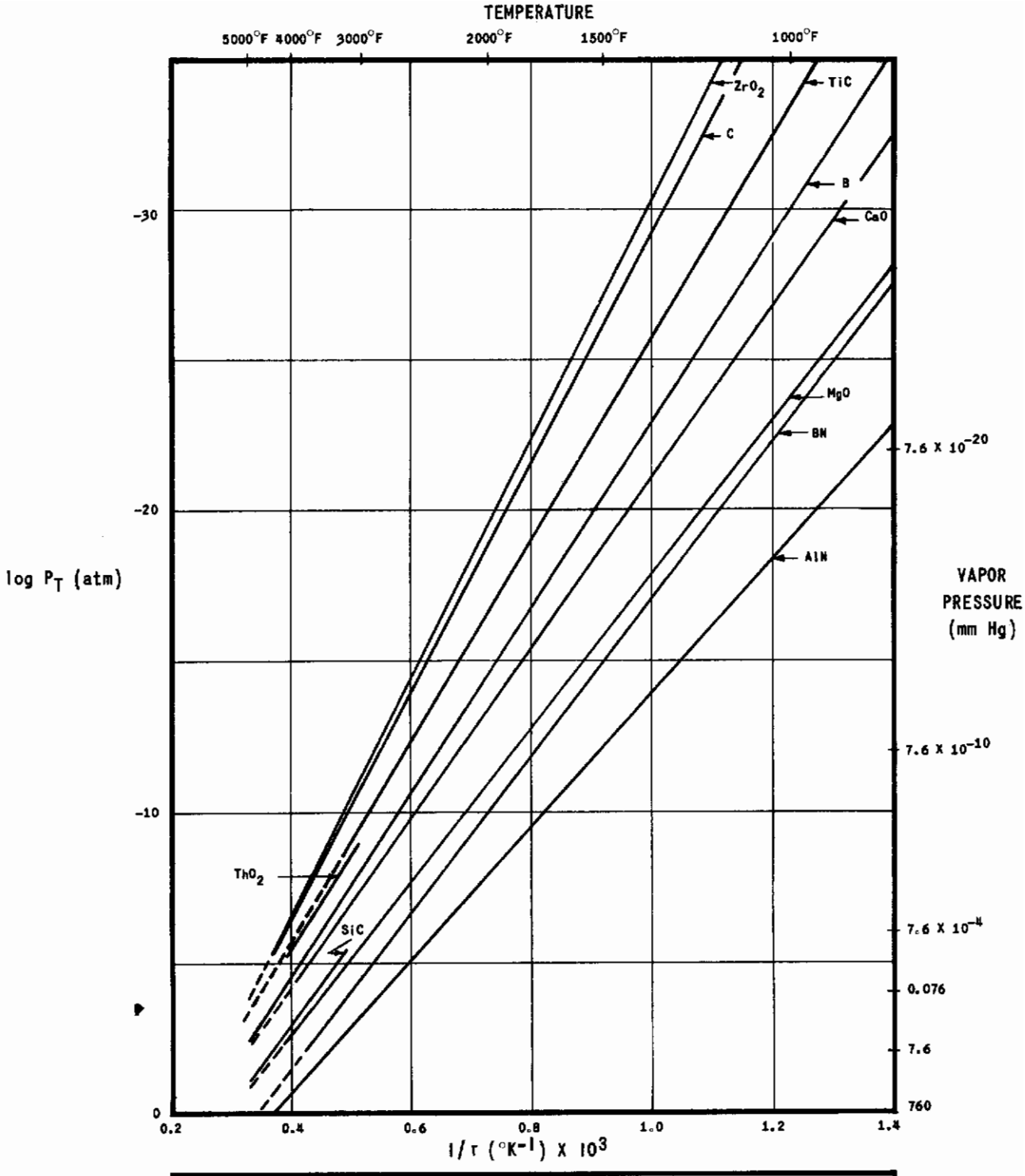

FIGURE 1 | Vapor Pressure in Equilibrium with Insulating Materials

Approved for Public Release

Contrails

The theoretical densities of the materials with low vapor pressures vary from 2.26 gm/cm^3 for graphite to 10.03 gm/cm^3 for thoria. In the application where powdered or fibrous materials are used, the actual densities are in the range of 0.11 gm/cm^3 for fibrous graphite felt to 1.75 gm/cm^3 for thoria. Since techniques are currently becoming available for producing fibrous ceramics[4] of much lower densities, the high densities of several of the promising insulation materials were not considered sufficient cause to eliminate them from consideration if the materials possessed other desirable properties.

Materials useful for radiation shields at high temperatures in an evacuated space are: tungsten, tantalum, molybdenum, and columbium. Some of the physical properties of these materials are presented in Table II. Because of its ease of fabrication, its availability and its good strength properties at high temperatures[4a], tantalum appeared to be the most promising radiation shield material from the physical-property viewpoint.

3. Chemical Stability

Potential insulating materials must be chemically stable with their container. In an evacuated system they must also be compatible with each other, since some contact could occur by vapors diffusing through passages in the system.

Chemical stability is indicated by the absence of chemical reactions of insulation components maintained at high temperatures for prolonged periods of time. From thermodynamic principles, it is possible to calculate if a reaction will tend to occur between two solid materials placed in contact at specified temperatures. However, the rates of the reactions cannot be determined from these principles; they are usually determined by direct experimentation. For this reason, we have used both theoretical considerations and experimental data to evaluate the chemical stability of the insulation components.

Table III shows the temperatures at which reaction occurred between insulation materials and radiation-shield materials. These data are extracted from the experimental data reported in the literature.[5]

Table IV shows the results of theoretical calculations and experimental work performed during this investigation. (For details, see Second Semiannual Progress Report, January 10, 1961.) We obtained the experimental results by mixing powdered tantalum and the insulation component,

Approved for Public Release

Contrails

TABLE II

PHYSICAL PROPERTIES OF MATERIALS USEFUL AS HIGH-TEMPERATURE RADIATION SHIELDS

Metal	Melting Point (°F)	Density (gm/cm^3)	Vapor Pressure at 4000° F (atm)	Reference
Columbium (Niobium)	4530	8.55	---	(3)
Molybdenum	4710	10.2	2.7×10^{-7}	(1)
Tantalum	5400	16.6	1.1×10^{-9}	(1)
Tungsten	6100	19.3	1.7×10^{-10}	(1)

Approved for Public Release

TABLE III

REACTION BETWEEN INSULATION COMPONENTS IN VACUO

Combination	Lowest Temperature of Reaction (°F)	Type of Reaction	Remarks
C - W	2730	Carbide formation	
C - Mo	2730	Carbide formation	
C - ThO_2	3630	Reduction of thoria	Carbide at higher temperatures
C - ZrO_2	2910	Reduction of zirconia	Carbide at higher temperatures
C - MgO	3270	Reduction of magnesia	Some adherence
MgO - W	3630	Reduction of magnesia	Slight adherence
MgO - Mo	2910	Silvery deposits on magnesia	Erosion of molybdenum
MgO - ThO_2	3990	Vapor reaction	Thoria eroded but no adherence
MgO - ZrO_2	3630	Liquid phase	Specimens welded
ZrO_2 - W	2910	Yellow deposits at interface	Decomposition of zirconia at 4170°F
ZrO_2 - Mo	3990	Sintering apparent	Decomposition of zirconia at 4170°F
ZrO_2 - ThO_2	3990	Slight adherence	No liquid phase up to 4170°F
ThO_2 - W	3990	Slight thoria reduction	Little reaction up to 4170°F, adherence evident
ThO_2 - Mo	3450	Slight deposits with adherence	Little reaction up to 4170°F
Mo - W	3630	Slight adherence due to sintering	Greater adherence up to 4170°F

Reference: Johnson, P.D., J. American Ceramic Society, 33, 168 (1950)

Approved for Public Release

TABLE IV

REACTIONS BETWEEN INSULATION MATERIALS AND TANTALUM

Materials	Thermodynamic (Equilibrium) Considerations		Experimental Observations	
	Temperature (°F)	Reaction	Temperature (°F)	Reaction
Ta + ThO_2	4000	No reaction except at low pressures: $4Ta + 5ThO_2 \rightarrow 2Ta_2O_5 + 5Th$	3990	No apparent reaction; however, ThO_2 dark in color.
Ta + C	4000	TaC formation probable.	2640	Trace of TaC.
			2910	TaC formed.
			3270	TaC and impurities formed.
Ta + ZrO_2	4000	No reaction except at low pressures: $4Ta + 5ZrO_2 \rightarrow 2Ta_2O_5 + 5Zr$	2370	No apparent reaction.
			2730	No apparent reaction.
			3090	No apparent reaction.
			3270	No apparent reaction.
Ta + SiC	4000	Probable formation of TaC or Ta_2C.	2630	TaC and possibly $TaSi_2$.
			2910	TaC and impurities formed.
			3270	TaC and impurities formed.

Approved for Public Release

Confidential

Contrails

heating the mixture to high temperatures under moderate vacuum (10^{-4} to 10^{-5}mm Hg), and analyzing the resultant compounds by X-ray diffraction techniques. Although TaC is formed by the reaction of tantalum and graphite at high temperatures, this was not considered detrimental, since tantalum carbide itself is very stable at high temperatures (vapor pressure of 8×10^{-9} atm at 4000°F). However, the reaction between silicon carbide and tantalum is not desirable, since the silicon or other impurities formed would be vaporized.

The data in Tables III and IV indicate reactions that take place in a reasonable time period when the reactants are well mixed. In the thermal insulation system, contact between the insulation materials and the container or radiation shields is not intimate; therefore, the rates of the reactions given above are not expected to be high. In previous work in our laboratory, ADL-17 was found to be chemically stable in contact with inconel and stainless steel at temperatures up to 2000°F. Since the ADL-17 is used in the cooler parts of the insulation system, it was expected to be stable in contact with tantalum, a relatively unreactive material, at temperatures of at least 2000°F.

4. Sintering

The study of sintering phenomena carried out for many years has resulted in a variety of mechanisms that have been proposed to explain the experimental results. MacKenzie and Shuttleworth[6] proposed that plastic deformation motivated by surface stresses was the cause of density changes upon heating of metal powders; however, this mechanism has not been widely supported.

Vapor-phase transport of material and subsequent deposition resulting in shape and dimensional changes of powders has also been proposed. Experimental studies of neck formation between spheres and plates of materials have not given evidence to support this mechanism.[7] In most experimental observations on the early stages of sintering, in which well-defined geometrical systems are used, the rate of neck growth is found to be consistent with a process that depends upon volume diffusion.[8] A number of years ago, Kuczynski[9] postulated that neck growth with compaction during sintering may be described as the migration of vacancies from the surface in the vicinity of the neck to the boundary between particles. This postulate is based on the assumption that the surface in the vicinity of the neck is an ideal source of vacancies and that the grain boundary between the particles is an ideal sink. The rate-limiting process is the rate of diffusion between the two.

Approved for Public Release

Contrails

The available experimental data on the diffusion characteristics of oxides indicate that the diffusion kinetics are controlled by the concentration of lattice vacancies or interstitial ions that are capable of movement and by the ease of motion of these defects. If the parameters involved in preparing a powdered compound and its environment on heating are adjusted so that the concentration of point defects in the compound are minimized, the shrinkage rate and sintering rate will be reduced. Nonstoichiometry of the compound, impurities, and thermal history of the compound influence the number of vacancies. In addition, the composition and pressure of the environment will influence the vacancy concentration and the resulting sintering rate. Data in the literature indicate that these factors do not markedly influence the sintering rate at temperatures below 75% of the melting temperature on the absolute scale.(10)

In terms of our present understanding of the sintering process, and in view of the limited experimental data available on diffusion in refractory inorganic compounds, the higher the melting point and the more pure the compound, the less the possibility of sintering. The only materials in Table I that meet the melting-point criterion for the absence of sintering at 4000°F are titanium carbide, graphite, thoria, and boron nitride. Of the four, thoria and graphite are available in the most pure form.

Preliminary experimental observations (for details, see Second Semiannual Progress Report, January 10, 1961) on the shrinkage of refractory powders when heated indicated volume changes that were much larger than predictable by any sintering theory. It is probable that the shrinkage (up to 50% for graphite and thoria) of the powders was due to bulk movement and changes in the packing. This is especially reasonable since the powders were not tapped or packed before heating. In the final experiments, attempts were made to use powders of specific densities, which were determined by settling tests. In this way, compaction because of packing changes should be greatly reduced. Also, the thermal history of the powders were recorded, to account for any changes that may have been caused by temperature cycling.

5. Thermal Conductivity

Very little experimental data on the thermal conductivity of powdered insulation materials at high temperatures is available. Preliminary determinations of the thermal conductivity of graphite fibers, thoria, zirconia, and silicon carbide were made at various temperatures between 2000 and 3500°F. (The experimental equipment and a complete description of the method is given in the Second Semiannual Progress Report.) The experimental results

Approved for Public Release

Contrails

are summarized in Table V. The actual variation in the thermal conductivities of the materials is not very great in view of the observed variation caused by differences in density, particle size, or manufacturing procedures. The thermal conductivity of zirconia and silicon carbide increased at a constant temperature after the material was heated to a higher temperature. This was probably the result of sintering or compaction. Thoria and graphite showed a decrease in thermal conductivity under similar conditions. This may be explained by loss of impurities at the high temperatures.

6. Materials Chosen For Extensive Thermal Tests

The choice of materials for long-period, high-temperature tests was based upon the results of the investigations discussed above. ADL-17 was chosen for the cooler parts of the apparatus and thoria for the intermediate temperature zones. Graphite fibers were used in the high temperature zones of the insulation packages. These materials were studied more extensively with respect to physical and chemical stability, sintering, and thermal conductivity. Tantalum was chosen for both the insulation container and for the radiation shields.

C. EVALUATION OF MATERIALS

The selected materials were subjected to high temperature conditions for periods of several hours to over two weeks. Examination of the materials before and after heating, their behavior during heating, and the results of thermal conductivity measurements gave information on the chemical and physical stability of the insulation materials. The thermal conductivity tests are discussed at greater length in Section IV of this report. Only the interpretation of the results with respect to chemical and physical stability need be considered here.

Five series of tests will be considered in detail throughout the remainder of this report. The principal characteristics of these tests are shown in Table VI.

1. Physical Stability

Physical stability of the insulation materials is indicated by a comparison of the appearance, color, texture, weight, and thermal conductance of the material before and after heating.

Approved for Public Release

Contrails

TABLE V

RESULTS OF PRELIMINARY THERMAL CONDUCTIVITY TESTS

Material	Thermal Conductivity at: 2100°F (Btu/hr ft^2 °F/in.)	3500°F (Btu/hr ft^2 °F/in.)	Remarks
ZrO_2 (Fisher)[a]	0.6-0.7	2.6	k increased after heating.
ZrO_2 (Cabot)	0.5	---	
ZrO_2 (Monsanto)	0.1-0.2	0.33	k increased after heating; lowest value of k for ZrO_2.
ThO_2 (gas mantle)	0.5-0.55	0.8-1.1	k decreased after heating.
ThO_2 (precipitated)	0.4-0.9	1.1	k increased after heating.
ThO_2 (ashed cotton)	0.3-0.35	---	k decreased after heating.
SiC (low density)	0.55-0.65	0.95	k increased after heating.
SiC (high density)	0.3-0.7	0.8	k increased by factor of 2 after heating.
C (graphite fibers)	0.7-0.9	2.0	k decreased after heating.

a. Manufacturer or characteristic feature.

Approved for Public Release

TABLE VI

CHARACTERISTICS OF HIGH TEMPERATURE TESTS

Series	Insulation Materials			Tantalum Radiation Shields[a]			Temperature Range (°F)	Test Duration[b] (Hours)
	Type	Density (lb/ft^3)	Thickness (in.)	Type (in.)		Number		
B	None	--	--	.010 and .012		2	80 - 2430	44
C	Graphite Fibers	5.7	0.625	.010 and .012		2	80 - 3150	50
D	Graphite Fibers	4.3	0.625	.002		6	80 - 3360	52
E	Graphite Fibers	3.4	0.50	.002		3	80 - 2690	137
	ADL-17	13.0	0.125	.010		1		
					Total	4		
F	ADL-17	12.8	0.125	.010		1	80 - 3500	340
	Thoria	104	0.125	.012		1		
	Graphite	3.8	0.125	.0005		2		
					Total	4		

a. Does not include outer container or inside stainless steel wall.
b. Actual time during which insulation was at elevated temperatures.

Approved for Public Release

Contrails

a. Tantalum

The tantalum shields (.010 and .012 in.) and outer container had a dull finish before heating. After exposure to temperatures above 2500°F in the vacuum furnace, a shiny, low-emissivity surface resulted. Figure 2 shows the tantalum outer container after heating to 3300°F (magnification 8x). The dark spot is a hole to ease evacuation of residual gases. Upon prolonged heating at high temperatures (series C and D), and upon rapid cooling at the end of the series, grain growth and crystallinity were apparent in the outer tantalum container. Figure 3 shows an enlargement (magnification 9x) of the surface indicating these effects. Upon continued heating during tests E and F, the outer shield did not undergo additional changes. Tantalum which was in good contact with graphite showed chemical changes that will be discussed later. Aside from the appearance of the outer surface, the tantalum appeared physically stable at high temperatures. Its ductility was reduced, but its strength appeared unchanged. There was no apparent weight loss of the outer shield, and outgassing of the tantalum during heating was small.

b. ADL-17

After the completion of series E, the ADL-17 powder appeared to have undergone no significant changes in its appearance or physical properties. Figure 4, a photograph taken at the end of series E, shows an enlargement (magnification 11x) of the ADL-17 used in this test. The white material is alumina powder. The ADL-17 powder was packed into an annulus between the inside stainless steel tube and the inner radiation shield. (A description of the geometry of the test apparatus is given in Section IV of this report.) When it was removed, the powder retained the shape of the annulus, although it was very friable and could easily be changed to a low-density powder by vibration or any similar disturbance. The photo shows the shape of the powder and the cross section. (The thickness of the insulation was 0.23 in.) The cross section of the powder was uniform in appearance, indicating no changes due to exposure to high temperatures. In series E, the outside of the ADL-17 layer was exposed to temperatures of 2100°F for over three days. In our past work, ADL-17 remained physically stable at temperatures up to 2200°F for prolonged periods. ADL-17 outgassed to only a small degree upon heating.

Approved for Public Release

Contrails

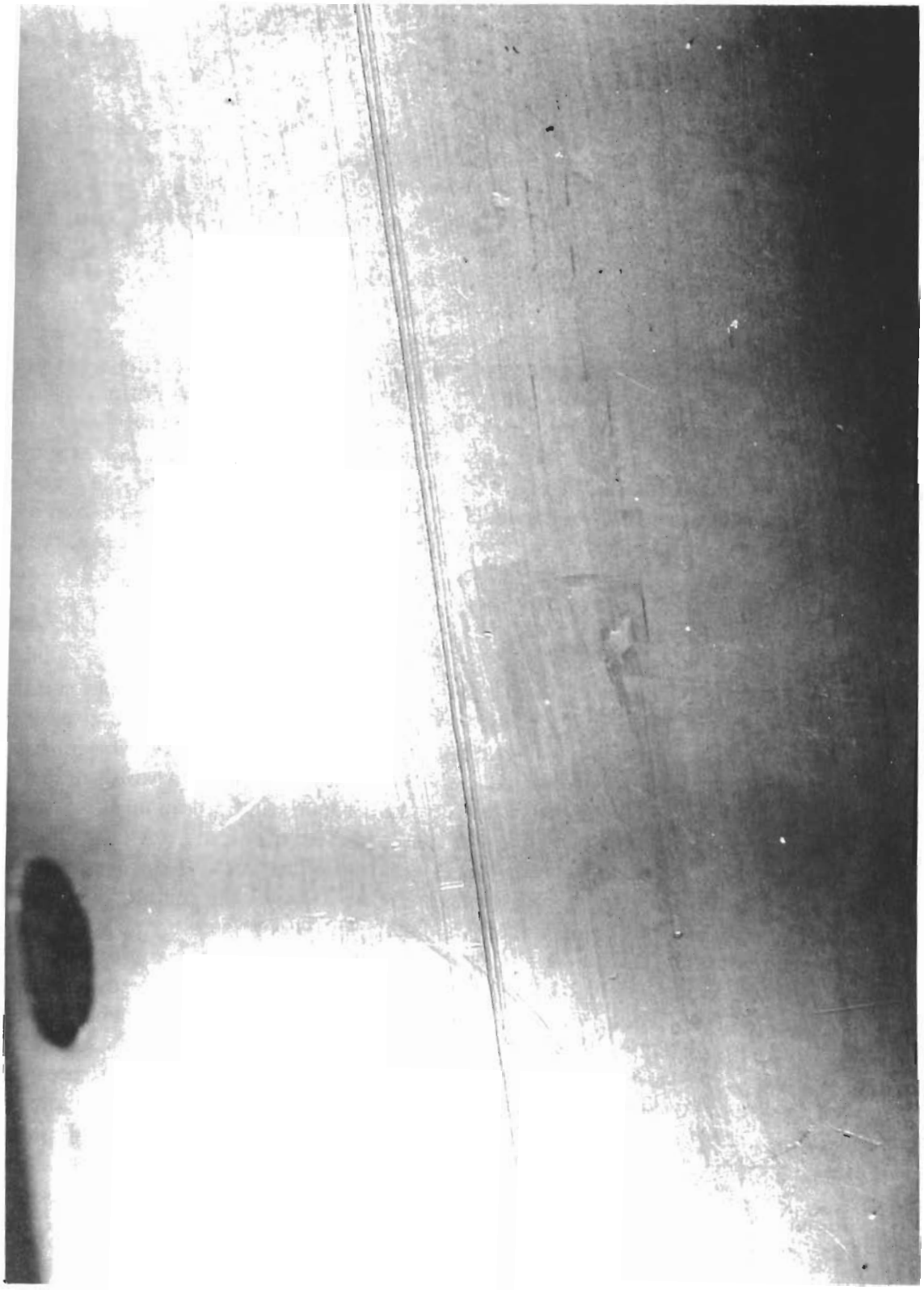

FIGURE 2 | Outer Tantalum Shield After Heating to 3300°F

Approved for Public Release

Contrails

FIGURE 3 | Outer Tantalum Shield After Prolonged Heating

Approved for Public Release

Contrails

FIGURE 4 | ADL-17 Powder After Heating to 2000°F for Several Days

Approved for Public Release

Contrails

c. Graphite Fibers

Graphite fibers changed slightly in color and appearance upon heating to 3300°F during tests C and D. The graphite felt was originally gray in color and had fairly strong tear resistance. Upon heating, the fibers that were in good contact with the tantalum and those that were in the hotter zones of the insulation system significantly darkened in color. Figure 5 shows the gradations in color caused by the contact with tantalum and the temperature gradients in the system. The graphite felt shown in Figure 5 was used in series E; it was rolled in a spiral fashion with tantalum shields spaced between the layers. Some parts of the felt showed small dark spots corresponding to holes in the radiation shields, indicating higher temperatures at these points. Fibers in test F had a similar appearance but were a brownish color. In addition to color changes, the fibers were more friable and had less tear resistance after heating. There was no significant weight loss or density change of the fiber matting after heating. It was surprising that even though the fibers had a large surface area, there was little outgassing during heating of the graphite.

d. Thoria

Prior to the heating procedure, the thoria was a fine, white, free-flowing powder. When the thermal conductivity apparatus was disassembled after heating in the tests of series F, the thoria had compacted and could be removed only with considerable difficulty. It was removed in chips and flakes varying in size up to 3/4 inch in diameter, and conformed in shape to the annulus in which it was packed. Figure 6 shows one of the thoria particles. Cracks in the surface extended approximately 1/3 through the particles. The chips were hard and difficult to crush. The thoria had also darkened slightly in color, especially where there was contact with the graphite at the evacuation holes.

2. Chemical Stability

Examination of the powdered insulation materials showed some evidence of reaction with other materials and the tantalum container.

Approved for Public Release

Contrails

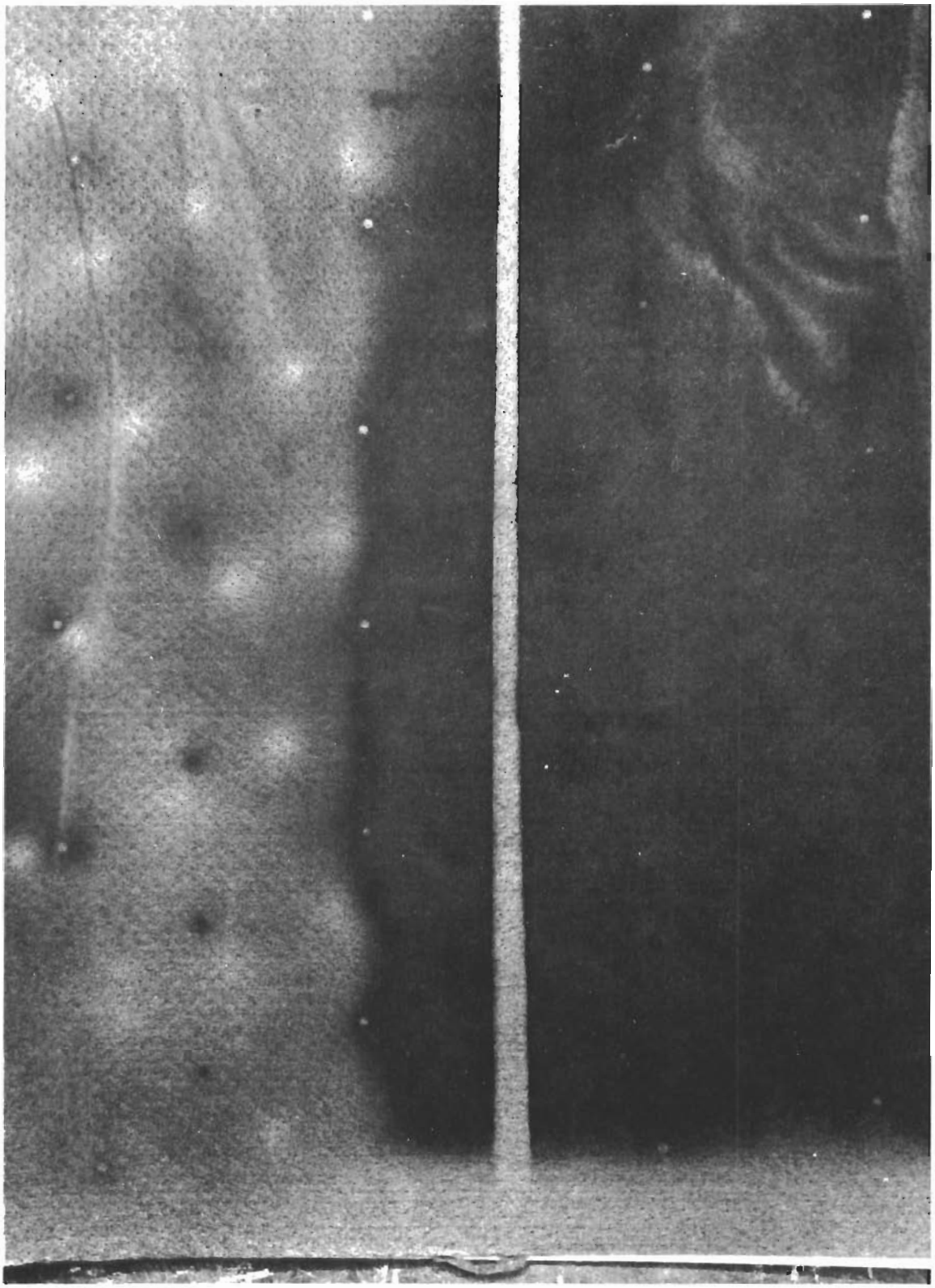

FIGURE 5 | Graphite Felt After Heating to 3300°F

Approved for Public Release

Contrails

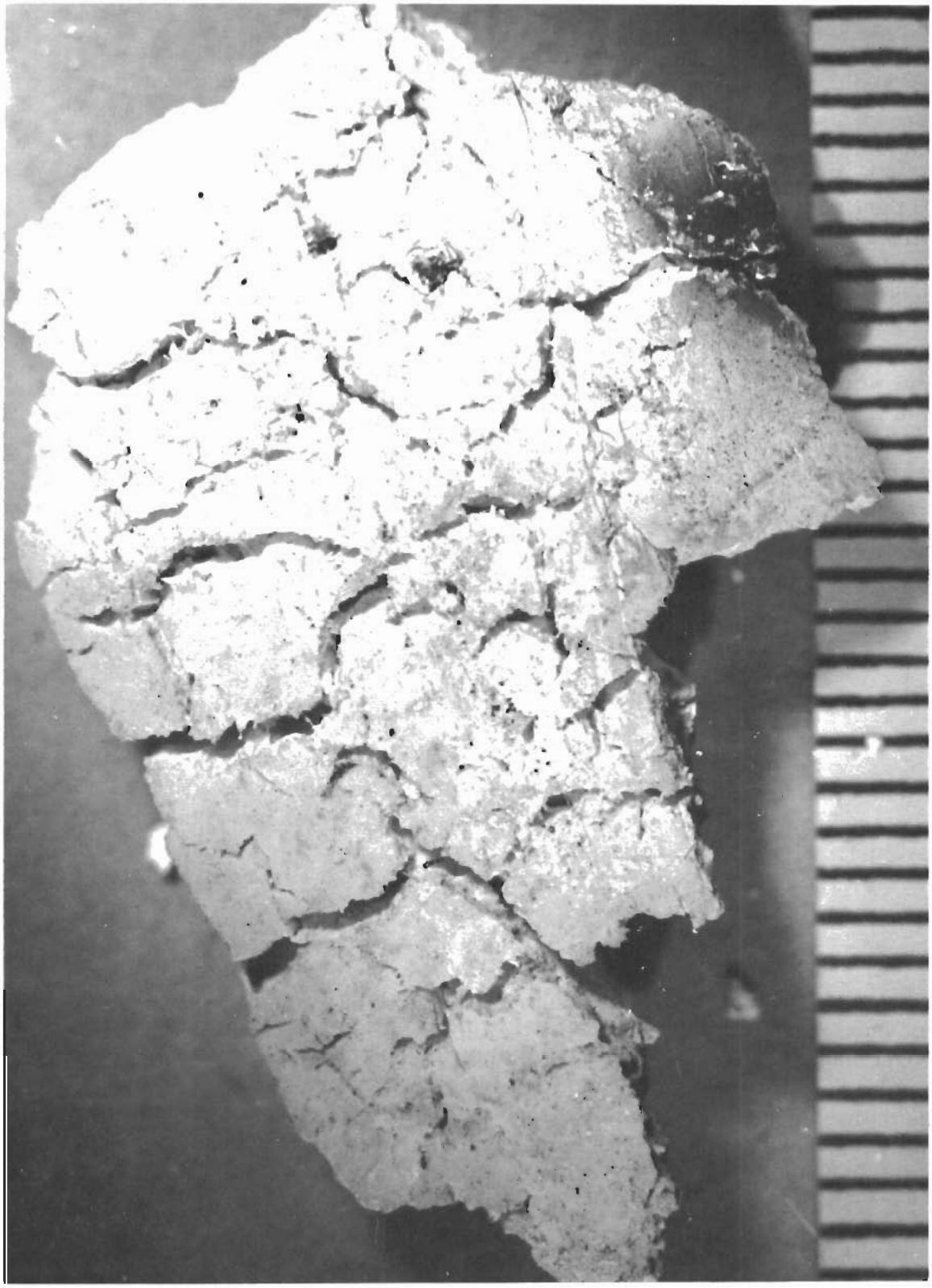

FIGURE 6 | Thoria Powder After Heating to 3200°F

Approved for Public Release

Contrails

a. Reactions of Insulation Materials and Container

After series E, the tantalum shields (.002 in. thick) in contact with ADL-17 and graphite turned dull gray in color, surface roughness increased, and surface emissivity apparently increased. The contrast between tantalum foil surfaces heated in contact with graphite fibers and unheated is shown in Figure 7. The dark area is the highly reflective unheated surface, and the light area is the dull gray surface after heating. Some short lengths of fibers adhering slightly to the surface may also be seen. The probable reaction was the formation of tantalum carbide. The tantalum shields were slightly embrittled but did not have any undesirable effects after heating in contact with the graphite in series B, C, D and E. In series F, in which 0.0005-in. shields were used, the tantalum foils turned golden in color, became very brittle, and broke into small flakes upon removal of the insulation from the apparatus. Figure 8 shows the fibers and the broken tantalum. Probably tantalum carbide was formed in larger quantities. It is possible that the thin tantalum foil was of different purity or surface characteristics than the heavier foil, even though both were obtained from the same manufacturer.

Thoria showed no evidence of chemical reaction with the tantalum shields.

b. Reactions Between the Insulating Materials

No apparent reactions took place among the components of ADL-17 at temperatures below 2000°F. In series F, the temperature of the ADL-17 increased to well above 2200°F, and some decomposition of the material resulted. Figure 9 shows the surface of the ADL-17 after heating for two weeks. The material turned gray and appeared to have reacted. There were also several cracks and fissures in the material.

The surfaces of contact of the other insulation materials, i.e., thoria and graphite, were very small. The only contact was at the evacuation holes in the radiation shields. Little evidence of reaction between the thoria and graphite was evidenced. Since the end plugs of the thermal conductivity apparatus were graphite, another opportunity was given to investigate the thoria-graphite reaction, although the temperatures at the ends of the apparatus were not as high as in the center. Again there was no evidence of reaction except for a slight darkening of the thoria.

Approved for Public Release

Contrails

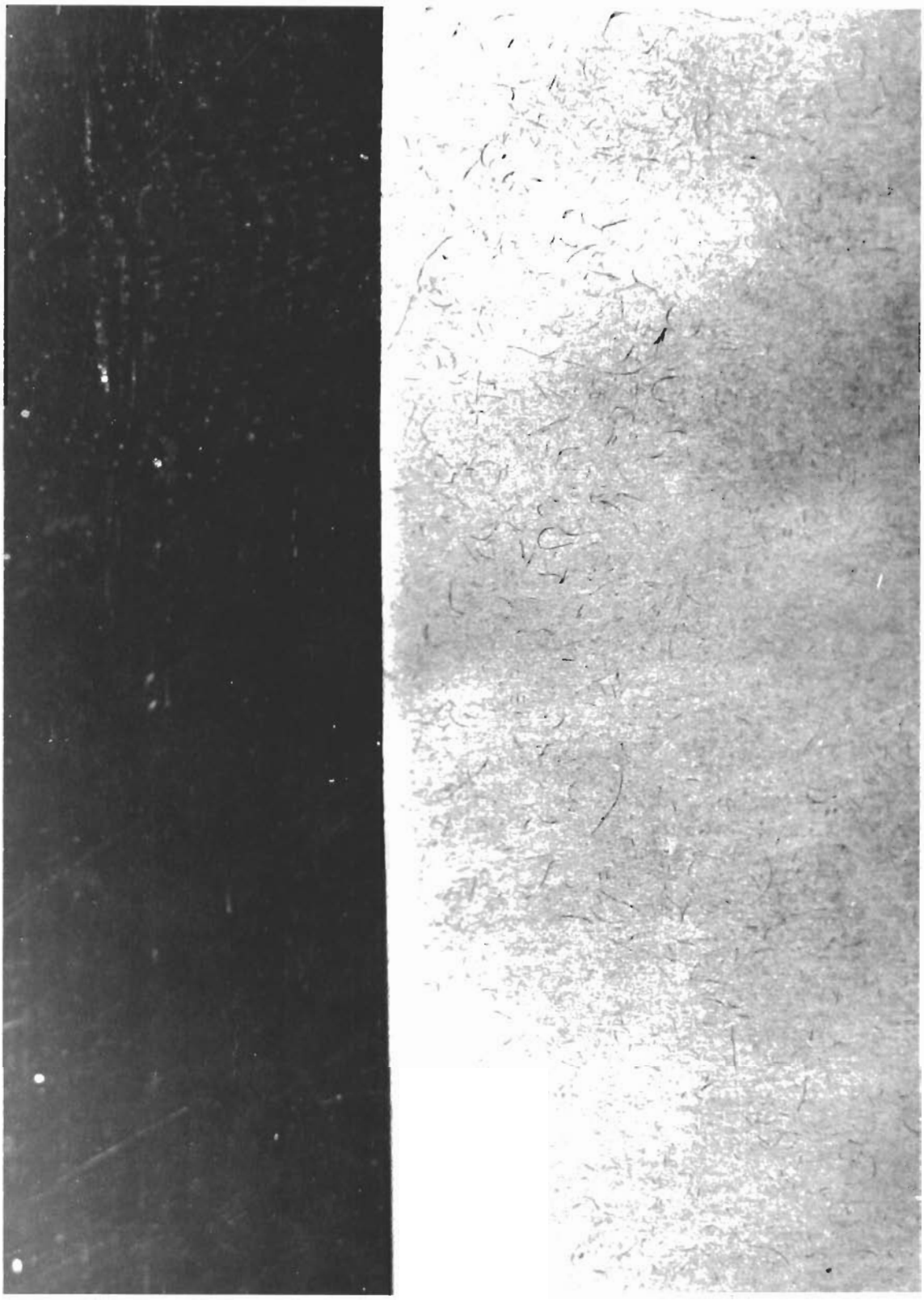

FIGURE 7 | Tantalum Shield Before and After Heating in Contact With Graphite Fibers

Approved for Public Release

Contrails

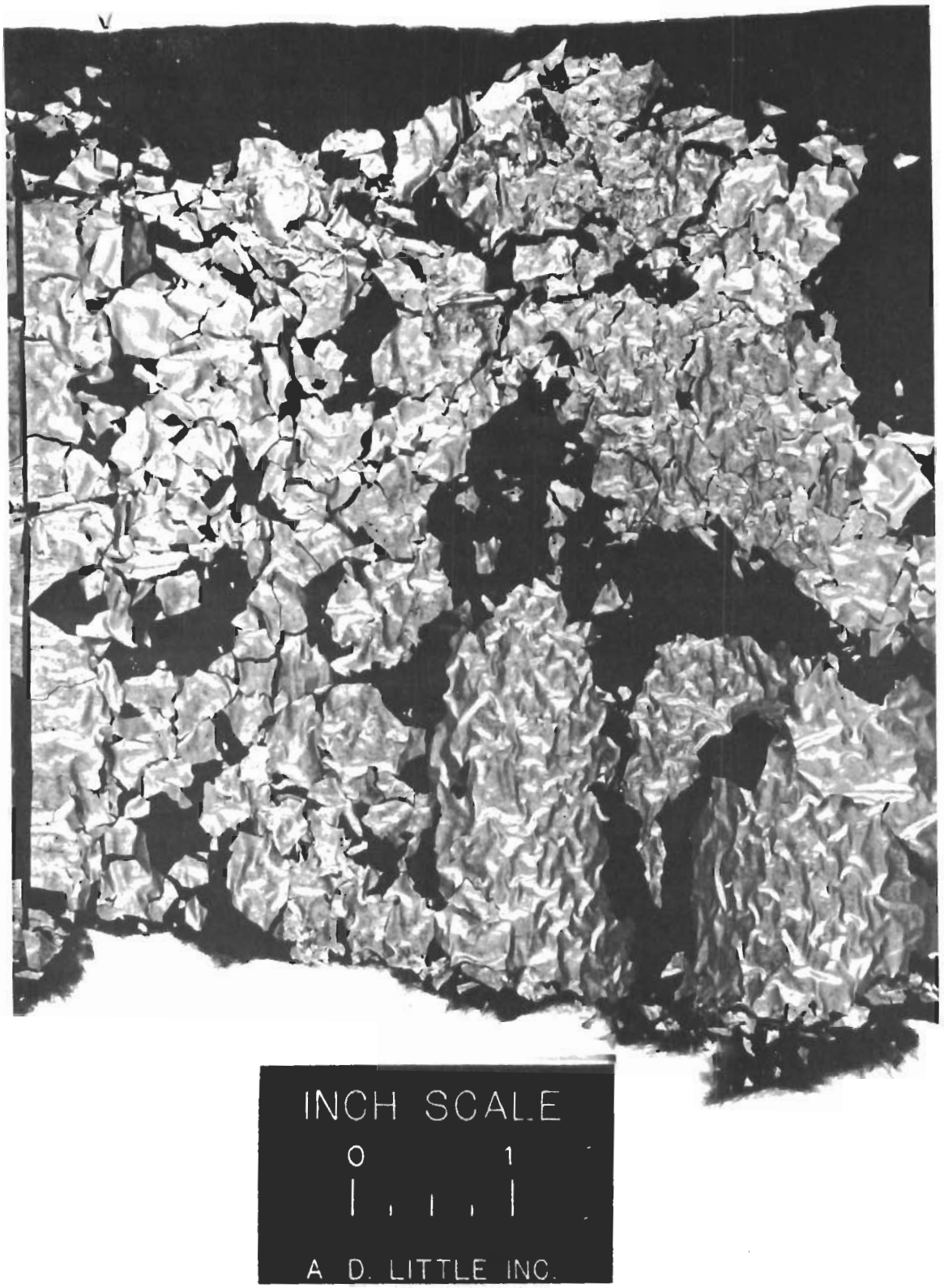

FIGURE 8 | Thin Tantalum Shields After Prolonged Heating in Contact with Graphite

Approved for Public Release

Contrails

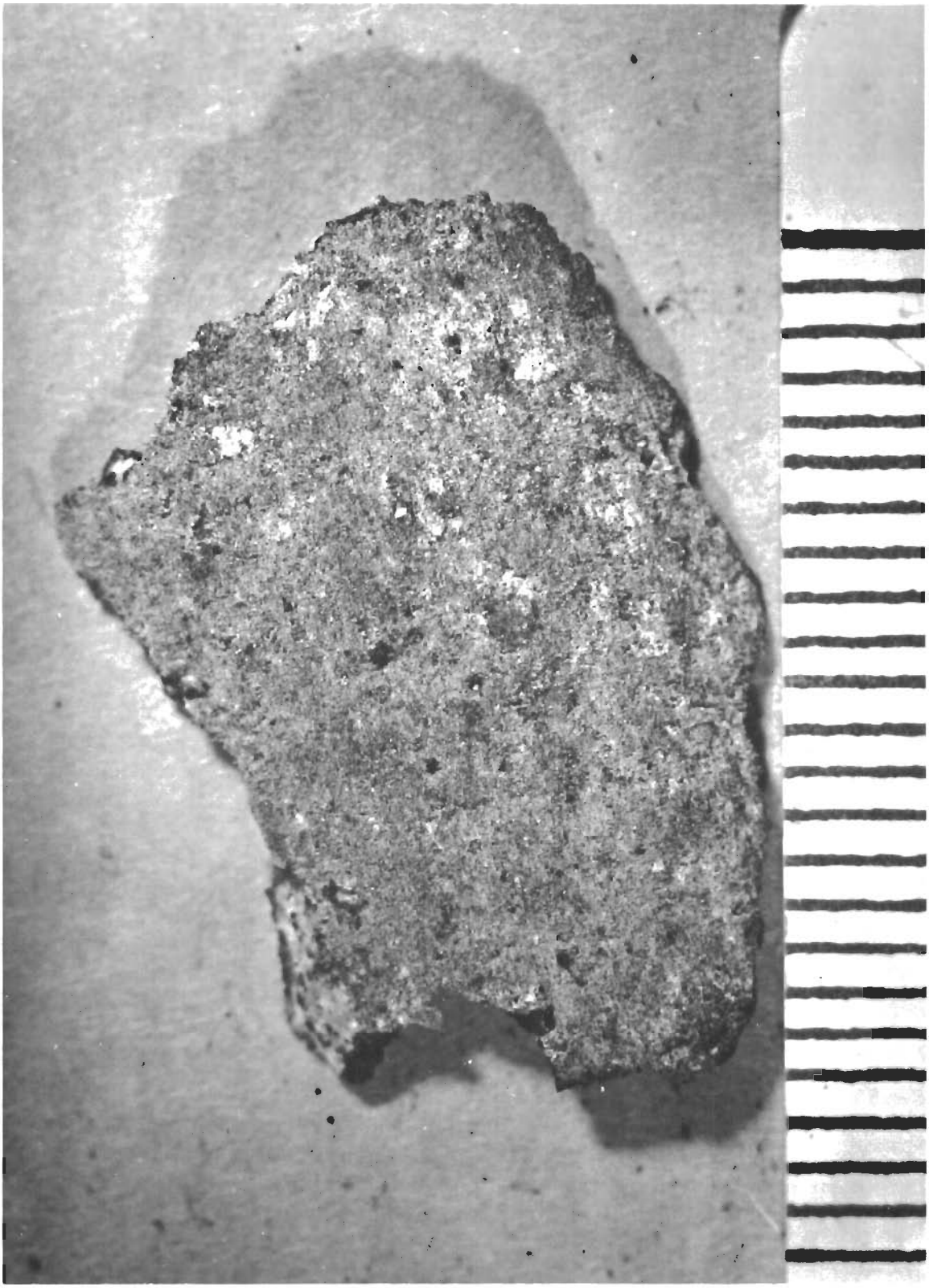

FIGURE 9 | ADL-17 After Heating to Over 2200°F for Two Weeks

Approved for Public Release

Contrails

In the experiments of series C, tungsten-rhenium thermocouples, insulated with alumina, were placed within the graphite fibers to measure temperatures of the system. At the end of series C, significant reaction was noted between the combination of materials (tantalum, graphite, and alumina). The alumina had eroded; a yellowish and black substance had formed; and the graphite and tantalum also had been attacked. The yellowish material may have been tantalum oxide. However, it may have also been the result of the reaction of alumina tantalum and rhenium of the thermocouples, as it is reported that tantalum-rhenium alloys form dark yellow oxides on reaction with air.[11] (Here, the Al_2O_3 would supply the oxygen.)

In several other tests--series B, D, E and F--alumina rods were placed in contact with tantalum (on the outside of the measuring device and on the furnace element) and heated to temperatures significantly higher than those in series C. There was no evidence of any reaction. Also, since alumina and carbon are intimately mixed in ADL-17, and since no reaction is evident between this mixture and tantalum, it is likely that the tungsten-rhenium couple is the cause of the reactions noticed in series C.

3. Sintering

In all the test runs there was no direct evidence of compaction or sintering of the ADL-17 or the graphite fibers. In series C and D, the graphite fiber mat, which has a thickness of approximately 0.10 in., was compressed to approximately 0.070 in. when it was placed in the thermal conductivity apparatus. After the graphite mat was removed at the end of the tests, measurements indicated that the thickness had increased to approximately .095 in. This change is not appreciable in view of the normal variation in thickness of the graphite matting.

Thoria, on the other hand, showed a large degree of compaction; because of the strength of the particles, it is expected that the powder sintered.

4. Long-Term Stability

The physical and chemical stability of the insulation materials is also indicated by the results of thermal conductivity measurements made during prolonged heating periods. In series E, for example, the effective thermal conductivity of the radiation shield combination of ADL-17, graphite, and tantalum varied only 4% over a period of 63 hours at a hot-wall temperature

Approved for Public Release

Contrails

of 2600°F. If any chemical or physical changes took place within the material, the thermal conductivity also would have changed. Similarly, in series F, only a 2% change was noted over 55 hours at 2400°F. At higher temperatures there were appreciable changes in thermal conductivity with time. Other implications of the results of the thermal conductivity tests are discussed later.

5. Discussion

On the basis of the experimental evidence presented above, the materials principally studied in this investigation (thoria, graphite fibers, ADL-17, and tantalum) fulfill most of the criteria for efficient insulation materials. They are physically and chemically stable enough to retain their thermal properties when used in proper combination in insulation systems at temperatures up to 3000°F for extended periods of 100 or more hours. At higher temperatures, sintering and compaction of thoria and reactions between graphite and tantalum would limit their use as thermal insulators to only several hours. It is possible that with pure thoria in the form of fibers, sintering would be greatly reduced, and the high-temperature insulating effectiveness extended. The degree to which these materials fulfill other criteria of efficient insulators will be discussed in the following sections.

Approved for Public Release

Contrails

III. HEAT TRANSFER THROUGH INSULATION MATERIALS

This section reviews the mechanisms of heat transfer through insulation materials to give a theoretical basis for methods of reducing heat transfer. The use of the effective thermal conductivity for describing the thermal characteristics of an insulation material will be discussed. High-temperature thermal conductivity tests performed in this investigation will be described and their results analyzed.

A. MECHANISMS OF HEAT TRANSFER

In insulating materials, the normal mechanisms of conduction, convection, and radiation contribute to the over-all rate of heat transfer in varying degrees, depending upon the temperature and pressure of the system and the properties of the specific materials. Although the mechanisms are interconnected, it is informative to consider them separately and determine which parameters significantly influence the rate of heat transfer by each mechanism . If methods of reducing the rate of heat transfer by each mechanism can be deduced, we can use this information as a basis for determining the over-all rate of heat transfer.

1. Solid Conduction

Heat is transferred by solid conduction in a powdered or fibrous material because of contact between the particles or fibers. Several investigators have shown that at higher temperatures, the rate of heat transfer by solid conduction is only a small portion of the total heat transfer rate.[12, 13] Nevertheless, when heat transfer by other mechanisms is reduced, solid conduction becomes more influential. Methods of reducing heat transfer by solid conduction are: (1) to reduce particle contact area; (2) to increase the number of "high-resistance" contacts; and (3) to lengthen the direct conduction paths in the insulation material. These conditions are best met by the use of small particles or fine fibers as the insulation material. In general, the lower the density of the powder, the less the solid conduction. Other difficulties, however, such as high-radiation heat transfer and poor strength properties, usually accompany the use of low-density materials.

Approved for Public Release

Contrails

Another factor that affects the conduction heat transfer is the load applied to the insulation. Forces exerted on the insulation media increase particle or fiber contact area and therefore increase the heat-transfer rate due to conduction. For random arrangements of particles or fibers, the relationships between applied load and the heat-transfer rate due to solid conduction are difficult to evaluate; however, two examples may be given for simple arrangements of fibers and spheres. For a symmetrical array of fibers arranged in parallel planes, Strong, et al., [12] have shown that the heat-transfer rate per unit area perpendicular to the layers of fibers is:

$$q_c = \frac{4\pi R_F^3 \, k_F}{R_F \ln\left(\frac{4 R_F}{\Delta R_F}\right) + \ell} \frac{n\Delta T}{\Delta X} \qquad (4\text{-}1)$$

where R_F = fiber radius

k_F = thermal conductivity of material comprising fibers

n = number of fiber junctions per unit area

ℓ = distance between fiber junctions

ΔT = temperature rise in thickness ΔX of fiber mat

and $$\Delta R_F = 0.32 \, (S/E)^{2/3} \, R_F^{-1/3} \qquad (4\text{-}2)$$

where S = load per fiber contact

E = modulus of elasticity

The usual concept of an effective thermal conductivity can be used for this analysis derived for one dimensional heat flux, and equation 4-1 may be written as:

$$q_c = k_{c,\,eff} \frac{\Delta T}{\Delta X} \qquad (4\text{-}3)$$

where $k_{c,\,eff}$ the effective thermal conductivity for conduction through a fibrous mat is given as:

Approved for Public Release

Contrails

$$k_{c,\,eff} = \frac{4\,\pi R_F^3\; k_F\; n}{R_F + \left(\ln \frac{4\,R_F}{\Delta R_F}\right) + \ell} \qquad (4\text{-}4)$$

From equation 4-1 or 4-3, the general trends of heat transfer by conduction through the fibers may be seen. The smaller the fiber radius and the fewer fiber contacts, the smaller the heat flux. Also, the conduction heat transfer is a complex function of the loading on the fibers.

For a powder composed of uniform-diameter spherical particles of "open packing," with one-dimensional heat flow through the bed of powders, the effect of applied pressure on the solid-conduction heat transfer (see Appendix A) is given as:

$$k_{c,\,eff} = \frac{3\,\pi\,ks}{8} \left[\frac{3}{E}\,(1 - \nu^2)\,F\right]^{4/3} \qquad (4\text{-}5)$$

where k_s = thermal conductivity of spheres

ν = Poisson's ratio

F = load per unit area

It can be noted from equation 4-5 that the effective thermal conductivity is independent of the size of the spheres and increases with the force per unit area. For more complex arrangements of spheres, the size of the particles will influence the effective thermal conductivity.

2. Gas Conduction

In fibrous or powdered material, heat transfer by gas conduction may be a significant portion of the total heat transfer. Consideration of the effects of collisions of gas molecules with each other and with the surfaces of an insulation material leads to the following relationships between the thermal conductivity of a gas in a large space and that of a gas in a space filled with particles (see Appendix B):

Approved for Public Release

Contrails

$$\left(\frac{k_p}{k_{p_o}}\right)_T = \frac{\bar{x}}{1+\bar{x}} \tag{4-6}$$

where $$\bar{x} = \frac{Pd}{P_o L_{g_o}} \left(\frac{T_o}{T}\right)^{n+1/2} \tag{4-7}$$

P = gas pressure within voids of particle bed

L_{g_o} = mean free path of gas molecules at T_o, P_o

d = average distance a molecule can travel before collision with a solid barrier

T = absolute temperature

n = constant[20]

Subscript "o" indicates reference pressure and temperature. The value of "d" can be estimated from consideration of the size of the particles and their shape and type of packing, or by experimental techniques.

From these equations, it can be seen that lowering the gas pressure and reducing the space between collisions (best accomplished by reducing particle size) are effective methods of reducing heat transfer by gas conduction.

Figure 10 shows the relationships of equation 4-6 and 4-7 for the example of a powder composed of homogeneous incompressible spheres of intermediate packing density. It is seen that for powders of small particle size, only a moderate vacuum is needed to reduce heat transfer by gas conduction to a low level.

Approved for Public Release

Contrails

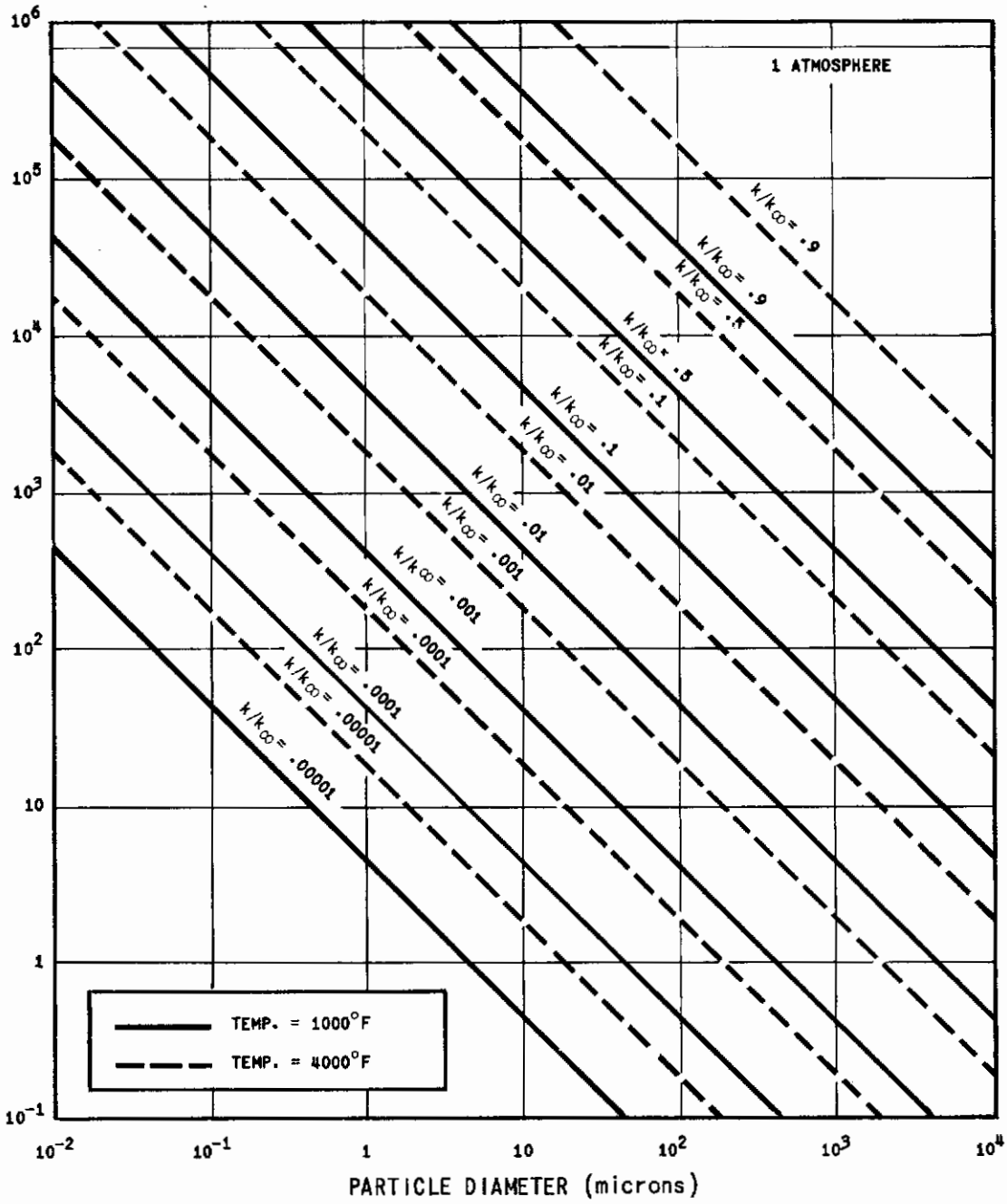

NOTES: 1. Pressure vs particle size required for various reductions in gas conductivity for powder composed of homogeneous incompressible spheres (intermediate packing).

2. k_∞ -- Conductivity of air at 1 Atm and temp. of k in large space.

FIGURE 10 | Effect of Pressure on Particle Size at 1000°F and 4000°F

Approved for Public Release

Contrails

3. Convection

In powdered or fibrous insulation materials, especially in evacuated systems, gas convection is negligible, and its contribution to heat transfer can be neglected.

4. Radiation

Heat transfer by radiation is an important mechanism in powdered or fibrous material, especially at higher temperatures. Several treatments of this subject are available in the literature.

MacAdams[14] cites the results of Damkohler, giving the contribution of radiation to the effective thermal conductivity as:

$$k_R = 0.692\ \delta D_p \frac{T^3}{10^8} \qquad (4\text{-}8)$$

where δ = void fraction

D_p = particle diameter (ft)

T = temperature of particles (°R)

By considering the radiation through voids between opaque particles in combination with radiation heat transfer between particles and solid conduction through the particles, Schotte[15] gives the radiation contribution to effective thermal conductivity as:

$$k_r = \frac{1 - \delta}{\frac{1}{k_s} + \frac{1}{k_r^o}} + \delta k_r^o \qquad (4\text{-}9)$$

where: $$k_r^o = 0.692\ \varepsilon \frac{D_p T^3}{10^8} \qquad (4\text{-}10)$$

k_s = thermal conductivity of the solid

ε = emissivity of material

Approved for Public Release

Contrails

More sophisticated analyses include absorption of energy by the particles or fibers.

Verschoor and Greebler[13], on treating a fibrous material as successive plates of fibers perpendicular to the heat flow, conclude that the contribution of radiation to the over-all thermal conductivity is:

$$k_r = 2.74 \times 10^{-13} \frac{Tm^3 \, Lf}{\alpha^2} \qquad (4\text{-}11)$$

where Tm = the mean insulation temperature (°R)

Lf = average spacing between fiber plates

α = fraction of incident radiant energy absorbed by a single fiber plane

Strong[12] gives the effective thermal conductivity for randomly oriented fibers as:

$$k_r = \frac{\frac{16}{3} \pi R_F \sigma T^3}{(1 - \delta) \varepsilon} \qquad (4\text{-}12)$$

By considering absorption and scattering in a powdered or fibrous material confined by boundary planes of emissivity ε_o, it is shown (Appendix B) that the heat flux due to radiation is:

$$q_R = \frac{J^2 \sigma (T_o^4 - T_L^4)}{(P + 2N) \frac{L}{2} + \frac{2}{\varepsilon_o} - 1} \qquad (4\text{-}13)$$

where: J = index of refraction

P = absorption cross section

N = scattering cross section

L = thickness of insulation

T_o, T_L = absolute temperature of hotter and cooler boundary walls, respectively.

Approved for Public Release

Contrails

A discussion of the validity and approximations used in formulating equation 4-13 is given in Appendix C.

In general, it can be seen from the above equations that effective thermal conductivity for radiation heat transfer is not only a strong function of temperature, approximating a T^3 relationship, but also a function of the dependence of the absorption and scattering cross sections on temperature. Increasing the absorption or scattering by the powders and reducing the void volume tend to reduce the radiation heat transfer. If the absorption and scattering cross sections are independent of temperature, equation 4-13 can be extended to a system of thickness "L" consisting of "n" thin radiation shields of emissivity ε_o, separated by insulation spaces of equal thickness to give:

$$q_R = \frac{J^2 \sigma (T_1^4 - T_2^4)}{(P + 2N)\frac{L}{2} + (n-1)(\frac{2}{\varepsilon_o} - 1)} \qquad (4\text{-}14)$$

where T_1 and T_2 are the temperatures of the hot and cold end surfaces. Examination of equation 4-14 shows that inclusion of radiation shields in an insulating material helps reduce the heat transfer by radiation; however, the degree of reduction depends upon the scattering and absorption cross sections as well as on the emissivity of the shields.

B. USE OF EFFECTIVE THERMAL CONDUCTIVITY

The above analyses show that a good method of comparing the various modes of heat transfer and their contributions to the total heat transfer is by use of the effective thermal conductivity. In the experimental work described below, the over-all effective thermal conductivity of the insulation systems was calculated from the measured heat fluxes, hot and cold wall temperatures, and the geometry of the systems. The values of the over-all effective thermal conductivities may be associated with the average temperature of the system or the temperature of any particular region of the system. Since most interest is on the hottest part of the system, and since the over-all thermal conductivity is a strong function of temperature, we have chosen the hot wall temperature as a correlating parameter.

In the January 10 Progress Report, methods of obtaining values of the thermal conductivity as functions of temperature were discussed. These methods required knowledge of the temperature profile within the insulation materials when more than one component was used in the insulation system. In the experimental work, attempts were made to measure the temperatures of various parts of the

Approved for Public Release

Contrails

system with tungsten-rhenium thermocouples. Both the brittleness of the materials and the reactions between the couples and the insulation materials made the use of the thermocouples difficult and the indicated temperatures unreliable. In certain cases, however, information on the apparent thermal conductivity of the individual materials can be obtained, as will be described later. The use of the over-all effective thermal conductivity is still valid; and it is especially informative in determining the effects of prolonged heating on the insulation system and in comparing the measured rates of heat transfer with estimates based on theoretical considerations.

C. THERMAL CONDUCTIVITY MEASUREMENTS

1. Apparatus and Method

The high-temperature furnace and accessory equipment for thermal conductivity tests are shown in Figure 11. The final design is essentially the same as that given in previous progress reports.

Figures 12 and 13 show the thermal-conductivity-measuring apparatus. For clarity, the cooling coils and measuring coil within the inside tube are not included in Figure 13, which shows the components used in the Series F tests. The inner tube is Type 304 stainless steel, 3/4-in. OD x .049 in., and 50 in. long. To aid in evacuation of the system, holes are drilled in the inner tube and the openings covered with fine mesh screening. Evacuation holes are also drilled in the tantalum shields. The ends of the inner tube are water-cooled and are shielded by cooled copper disks. The radiation shields were of three types: preformed tubes .020, .013 and .010-in. thick; .002-in. foil; and .005-in. foil. The heavier shields served two purposes: to confine the insulation and to act as shields within it. The types of insulations and the number of shields used in the experiments were given in Table VI.

When the apparatus was filled with insulation material, the graphite felt was cut to the desired length and wrapped spirally, with tantalum foil radiation shields between the layers. Since the matting is available only in one thickness, and the heavy tantalum shields were fixed in size, only a few density arrangements were allowable if symmetry was to be preserved. To prevent compaction or flow during the heating cycle, the powdered materials were vibrated and tamped as they were added to the measuring device.

Approved for Public Release

Contrails

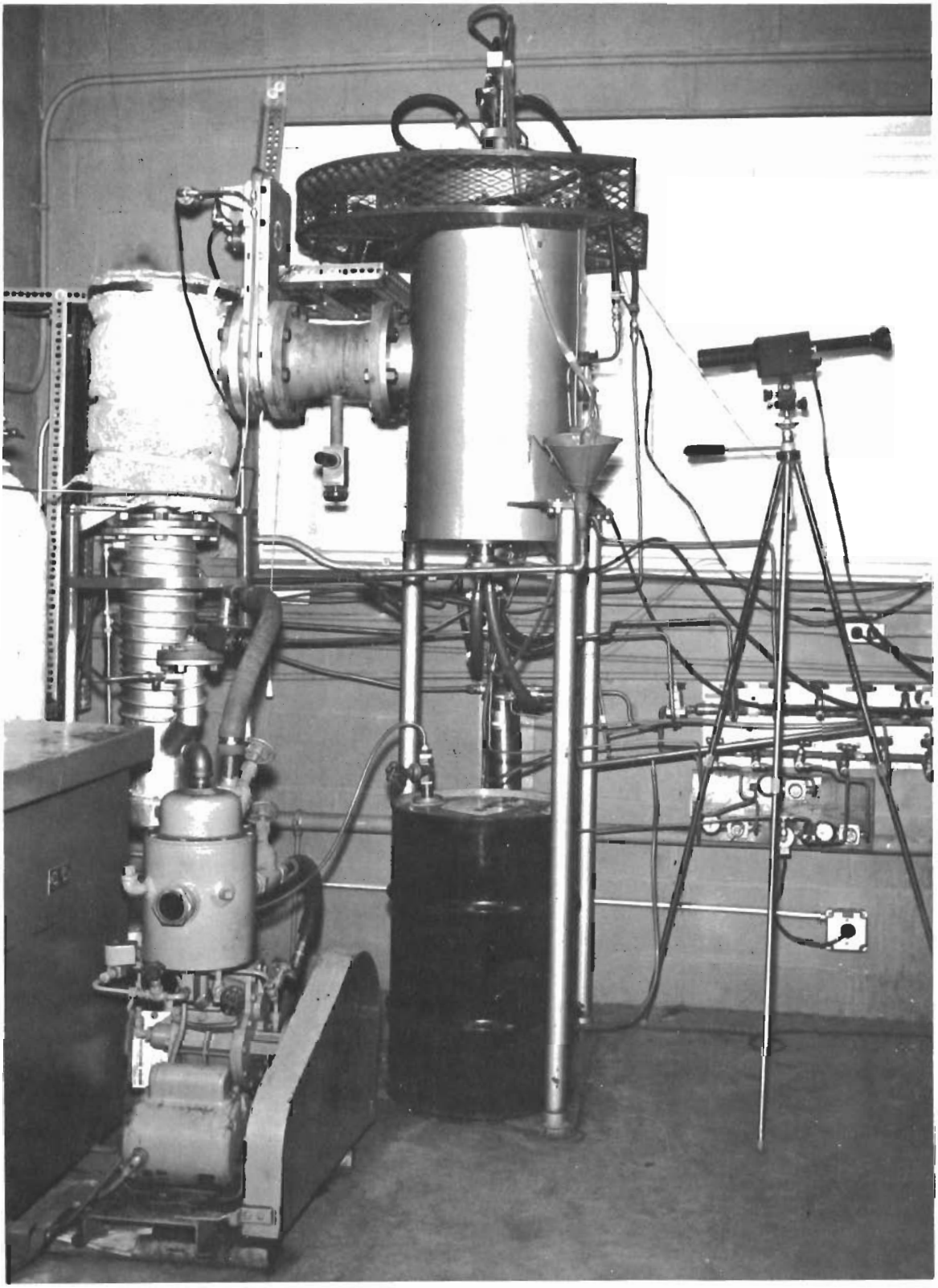

FIGURE 11 | High Temperature Furnace

Approved for Public Release

Contrails

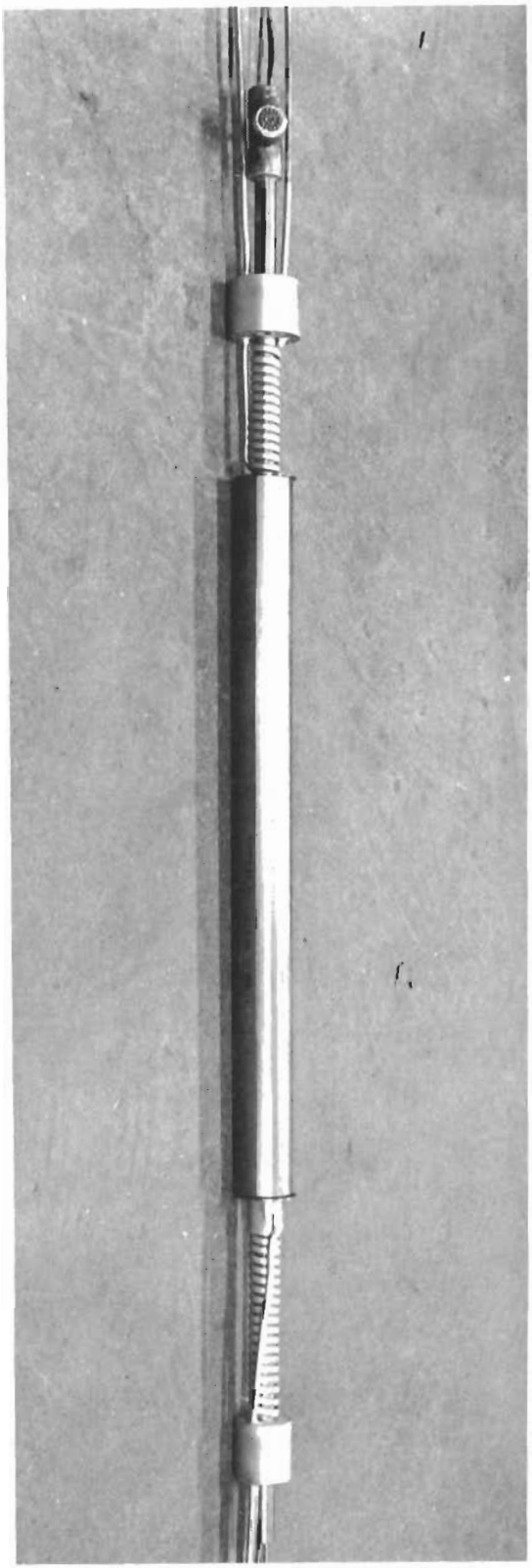

FIGURE 12 | Thermal Conductivity Apparatus

Approved for Public Release

Contrails

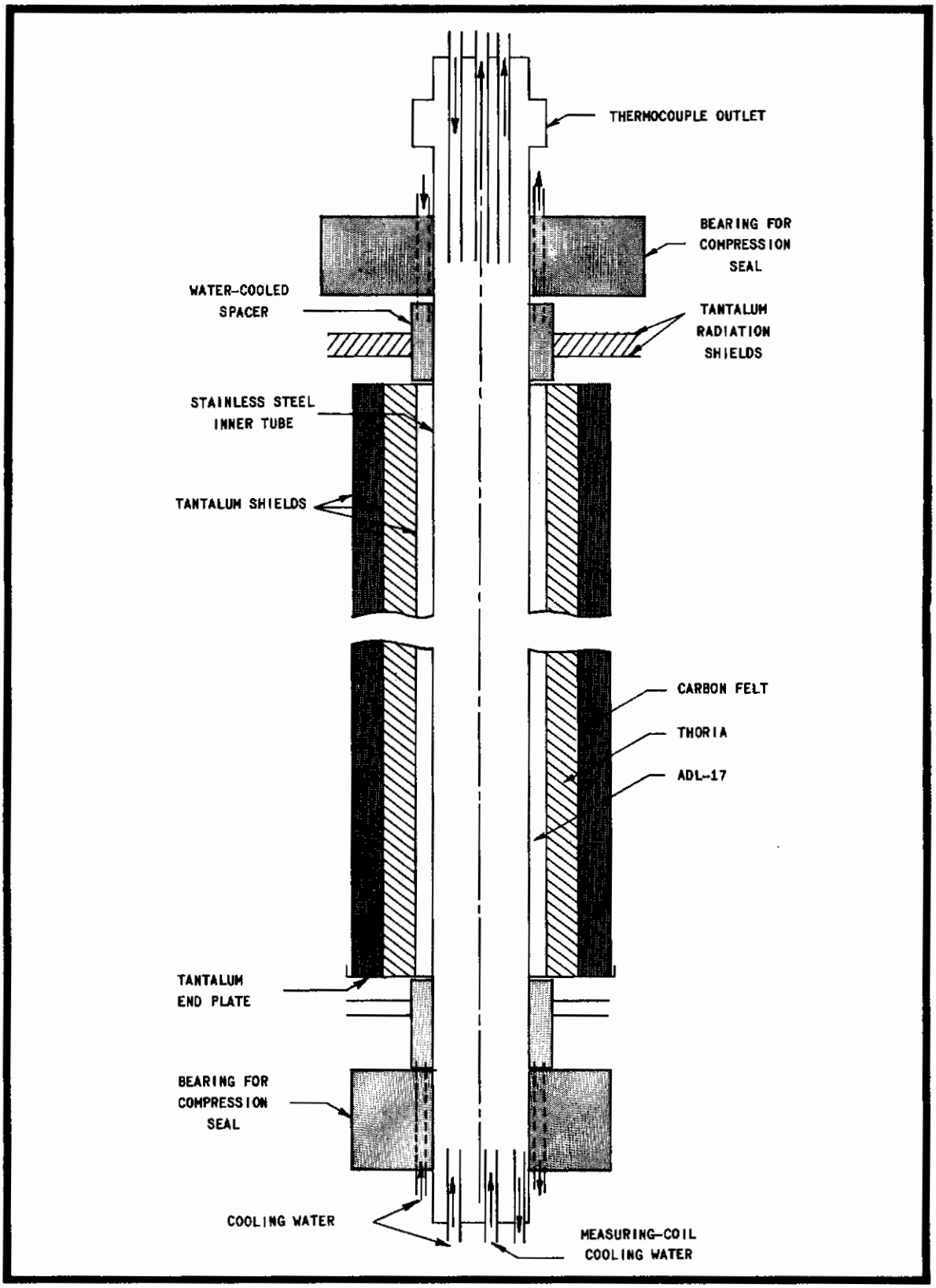

FIGURE 13 | Sketch of Thermal Conductivity Apparatus

Approved for Public Release

Contrails

When the device was filled, it was placed in the furnace chamber, which was evacuated slowly to prevent flow of the powdered materials.

In the initial experiments, the furnace was stopped after each day's operation. In subsequent tests, it operated for prolonged periods. The rate of heating was usually determined by the amount of outgassing, since it was desired to maintain a low pressure in the furnace chamber. Before any tests were made, the furnace remained undisturbed for two to twenty-four hours to insure temperature and pressure equilibrium. When the temperatures throughout the system were constant, steady-state conditions were assumed, and measurements were made.

In each run, the inlet and outlet cooling water temperatures, the cooling water flow rates, and the temperature of the outer shield were measured. Water temperatures were measured with a precision potentiometer, and recording potentiometers were used to show when temperatures were at steady values. The hot-shield temperatures were measured with thermocouples at the low temperatures and an optical pyrometer at higher temperatures. From these measurements the effective thermal conductivities of the insulation systems were calculated.

2. Reliability of Measurements and Estimate of Errors

a. Effective Thermal Conductivities

The temperatures of the outer shield (hot wall temperatures) are estimated to be reliable to within $\pm$ 1% at lower temperatures and $\pm$ 2% at higher temperatures. This was confirmed by the agreement of the optical pyrometer measurements with thermocouple measurements over the temperature range of 1200 to 2500°F. Because of the shape of the furnace and the sight port, the temperatures indicated by the pyrometer are "black-body" temperatures, and corrections due to emissivity of the outer shield are neglected. Corrections were made for absorption by the sighting window.

Changes in the flow rate of cooling water in the measuring coil were immediately reflected by changes in the temperature rise of the water. Since the heat flux is the important quantity, the possible error in the product of the flow rate and the temperature rise is important. At each temperature condition at least three determinations of the heat flux were made. These values always agreed within 5%; in most cases deviations were only 2%.

Approved for Public Release

Contrails

Another source of error is conduction loss in the inner stainless steel tube. During the measurements, temperatures at the ends of the guard coils were "matched" with those at the end of the measuring coil in order to reduce conduction losses. At the higher temperatures this procedure was more difficult, and some losses may have occurred. This would have the effect of lowering the measured effective thermal conductivity below the true value. Since tests at several temperatures were repeated with different flow rates and different degrees of matching, and since the effective thermal conductivities did not vary significantly, conduction losses appeared to give no appreciable error.

The estimated possible error of the thermal conductivity measurements is, therefore, estimated at less than $\pm$ 5% for temperatures below 2000°F and approximately $\pm$ 10% for higher temperatures.

b. Pressures

The pressures in the system were measured by an ionization gauge attached to the furnace chamber. Although these values accurately represented the pressures within the chamber, they were not necessarily the same as the pressure within the insulation material. During outgassing there was undoubtedly a substantial pressure gradient from the insulation material to the outside of the shields. After the materials remained at constant temperature for several hours, the furnace pressure was observed to be constant, and there was probably reasonable agreement between measured pressure in the furnace chamber and within the insulation material.

D. RESULTS OF THERMAL CONDUCTIVITY TESTS

1. Experimental Data

Figure 14 shows the experimentally measured values of the effective thermal conductivity for the materials system tested as a function of the hot wall temperature. In all tests the average cold wall temperature was approximately 110-130°F; the total insulation thickness (including shields) was 0.625 in. in all tests. Figure 14 also shows a calculated curve for a system consisting of three shields only, with the same geometrical arrangement as in series B. Calculations were made by standard techniques outlined by Hottel[17] and with emissivities given in the literature.[16] The pressure of the system during the thermal conductivity measurements varied from 3×10^{-7} to 5×10^{-5} mm Hg. Typical examples of the "temperature-time" and "pressure-time" relationships are shown in Figures 15 and 16 for series E and F, respectively. Effective thermal conductivities are also indicated.

Approved for Public Release

Contrails

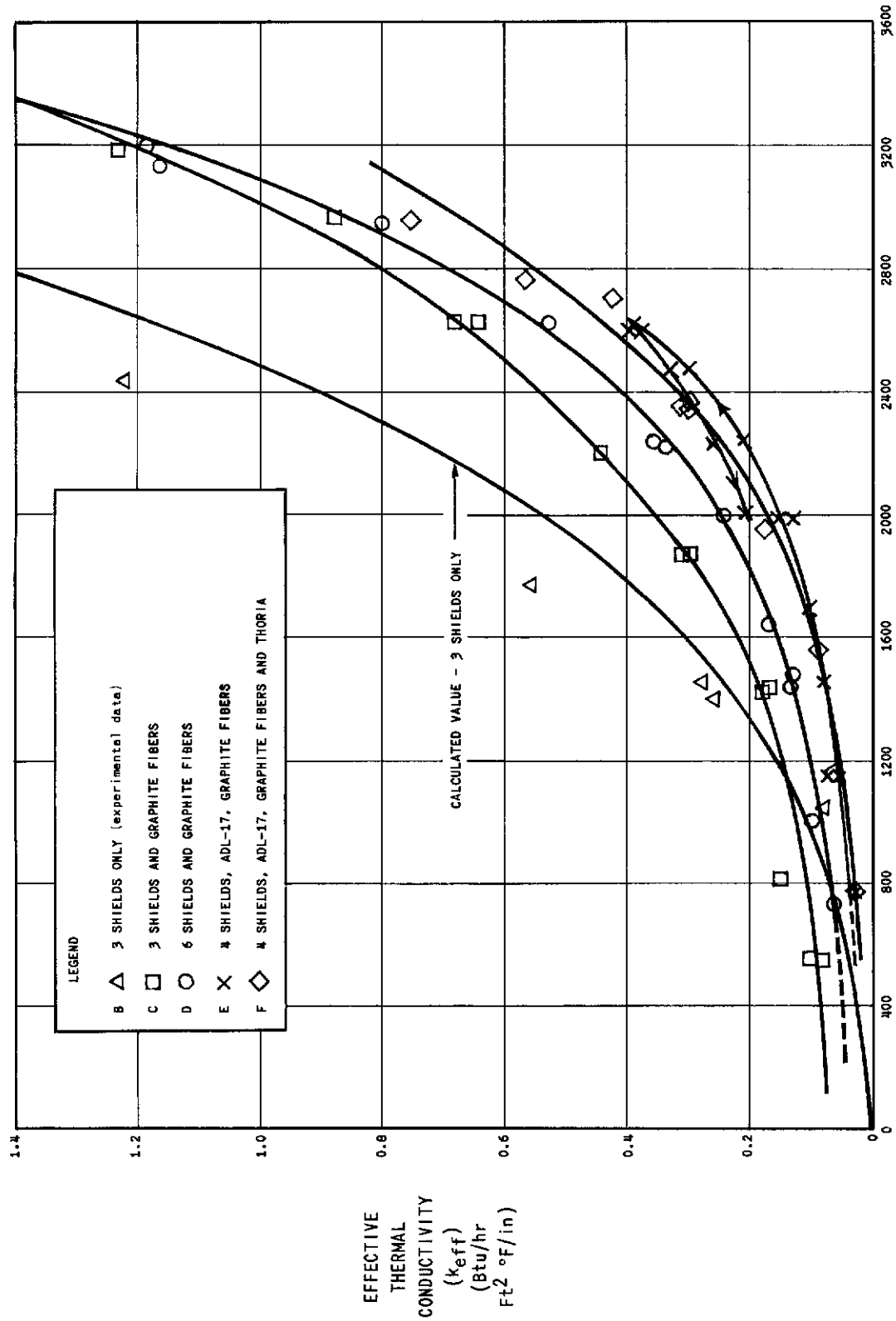

FIGURE 14 Effect of Hot Wall Temperature on Thermal Conductivity of Insulation Systems

Approved for Public Release

Contrails

2. Discussion of Thermal Conductivity Measurements

a. Effect of Pressure

Figures 15 and 16 show that during the periods of constant temperature, furnace pressure had little effect on the effective thermal conductivity of the materials. This indicated that gas conduction contributes a negligible amount to the total rate of heat transfer. A confirmation of this observation is found in the theories presented above. From the particle size of the insulation materials, the pressure required to reduce gas conduction to a small fraction of the free gas value can be found for the mean temperature of the insulation. Several typical values are shown below:

Material	Particle Size (microns)	Temperature (°F)	Pressure Necessary for Reduction of Gas Conduction to .001 Free Gas Value (mm Hg)
ADL-17	Less than 0.1	1000	4.4
		2000	8.60
Graphite Fibers	7.5	1000	1.2×10^{-3}
		2000	2.34×10^{-3}
		4000	5×10^{-3}
Thoria Powder	3	1000	.15
		2000	.29
		4000	.62

Although the pressures in the insulation material were probably greater than those indicated by the pressures in the furnace chamber, comparison of the measured furnace pressures with those given in the table above substantiates the conclusion that gas conduction was not an important heat-transfer mechanism under test conditions.

Approved for Public Release

Contrails

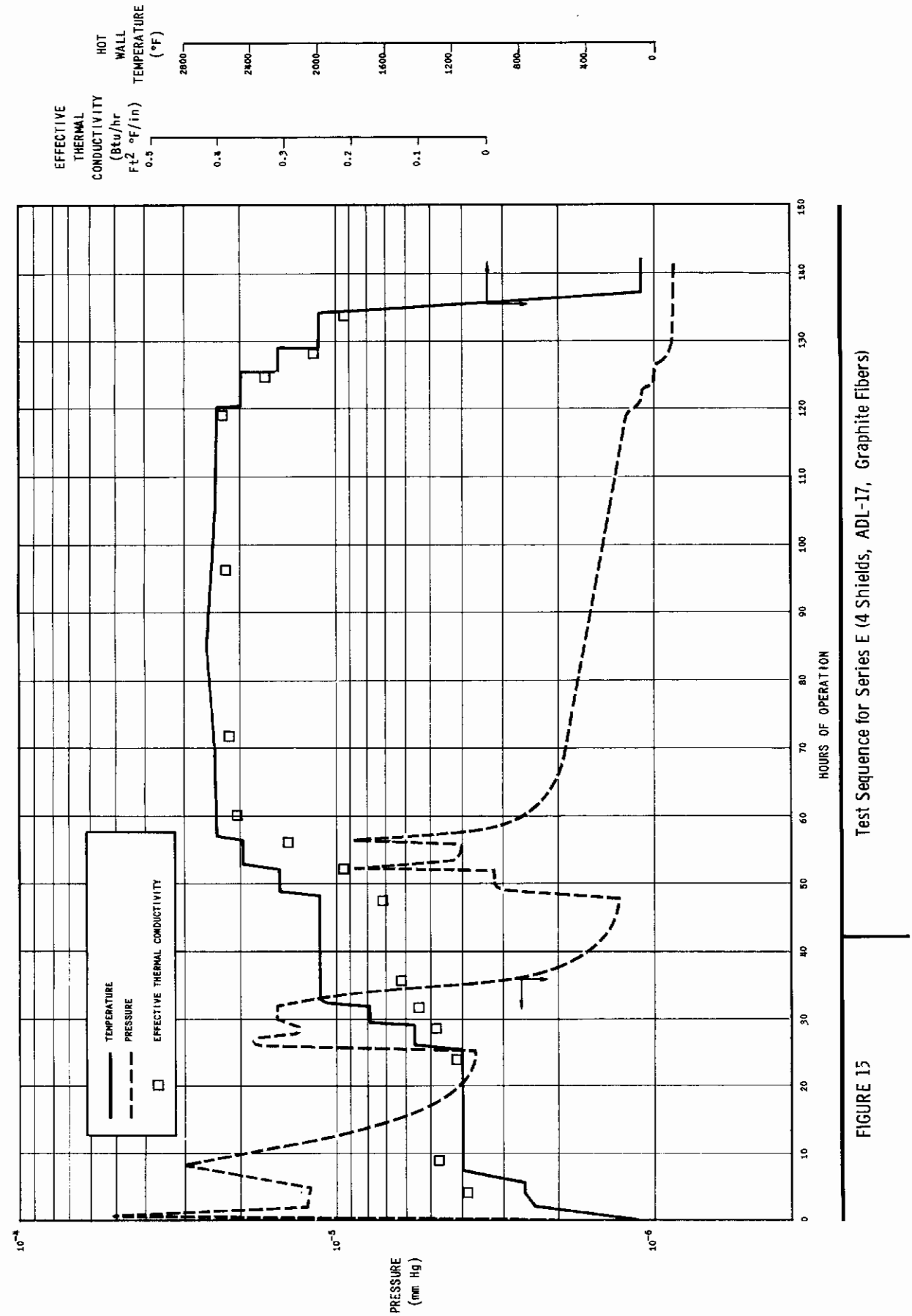

FIGURE 15 Test Sequence for Series E (4 Shields, ADL-17, Graphite Fibers)

Approved for Public Release

Contrails

As has been previously mentioned, the pressure within the furnace is an indication of the outgassing of the insulation materials. While the temperature of the insulation materials was being raised, some outgassing occurred; during the periods of steady temperatures, the outgassing decreased substantially. It should be noted that some of the gas released is from the furnace itself and not from only the insulation materials. The fact that outgassing occurred only during the initial heating period is of practical importance, since once the insulation material is "baked" at a high temperature, little outgassing will occur on subsequent heating cycles. An insulation package could be heated to a high temperature during its fabrication and not present outgassing problems during its actual use.

b. Effects of Temperature

It is evident from Figure 14 that the temperature of the insulation material has a predominant influence on the thermal conductivity. The theories presented earlier show that where radiation is the dominating heat-transfer mechanism, the effective thermal conductivity increases very rapidly with temperature and is approximately proportional to the cube of the mean temperature. In the systems considered in our work, there are very large temperature gradients through the insulation, and the mean temperature is substantially below the hot wall temperature. Since the thermal conductivity is such a strong function of temperature, it is expected that the hot wall temperature is a more reasonable parameter for describing the effects of temperature. This is also true from a practical standpoint, since in most applications the hot wall temperature, not the mean temperature, will be fixed.

Figure 17 also shows the thermal conductivities of the various insulation systems as a function of temperature. The effective thermal conductivities at higher temperatures are proportional to the absolute hot wall temperature raised to a power varying between 2.9 and 3.5. This indicates that above 1500°F, radiation is the most important mechanism for heat transfer and is in agreement with the theories presented earlier. Use of different insulation materials and numbers of shields does not change this proportionality. However, increasing the temperature range below which radiation heat transfer does not contribute greatly to the total heat transfer rate is beneficial.

Approved for Public Release

Contrails

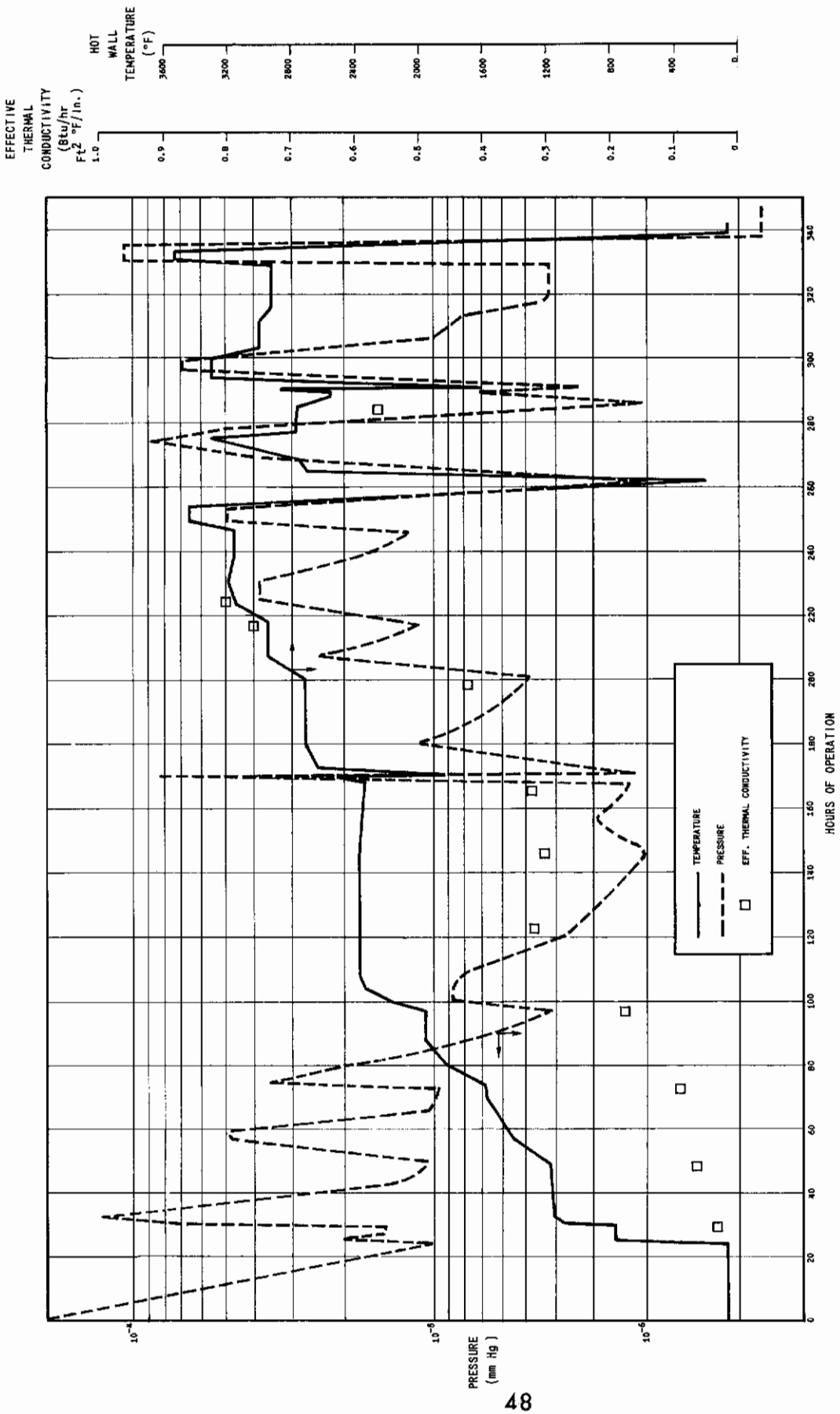

FIGURE 16 Test Sequence for Series F (4 Shields, ADL-17, Thoria, Graphite Fibers)

Approved for Public Release

Contrails

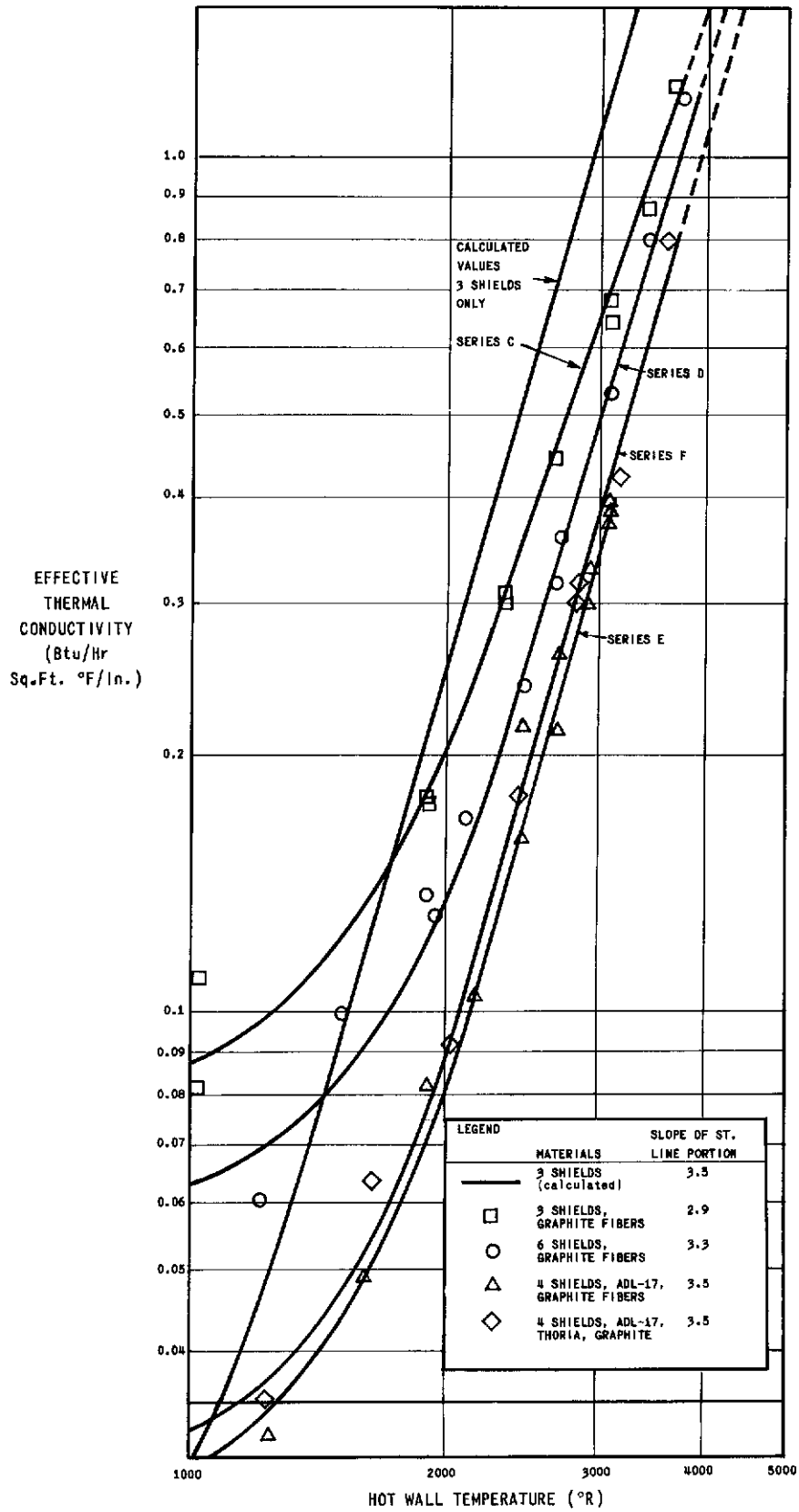

FIGURE 17 | Dependence of Effective Thermal Conductivity On Hot Wall Temperature

Approved for Public Release

Contrails

The combination of materials of series E--ADL-17 and graphite--has a lower thermal conductivity than the materials of series F--ADL-17, thoria, and graphite. Thoria must still be considered as an insulation component, however, since gas conduction can be eliminated in thoria powder at a higher pressure than in graphite fibers. This is of practical importance in the end use of the insulation material.

At a hot wall temperature of 2630°F for the materials of series E, the temperature of the radiation shield in contact with the ADL-17 layer was calculated to be 2150°F. This is close to the upper limit of operation of 2200°F found for ADL-17. Since the effective thermal conductivity of the materials of series F was higher than that of series E, for equal hot wall temperatures, the temperature of the shield contacting ADL-17 was higher in series F than in series E. Both the thermal conductivity data and examination of the ADL-17 show that the maximum useful temperature was surpassed in the higher temperature part of series F under prolonged exposure.

c. Effects of Density and Conduction Heat Transfer

Whereas the effective thermal conductivities of the higher temperatures reflect mainly the contribution of radiation heat transfer, the data at lower temperatures indicate the contribution of conduction heat transfer. Comparison of the low-temperature thermal conductivities indicates that graphite fibers are better conductors than combinations of ADL-17 or ADL-17 and thoria with graphite fibers. The difference in low-temperature thermal conductivity between series C and D is probably due to the lower density of graphite fibers used in Series D.

d. Effects of Radiation Shields

The effects of radiation shields are demonstrated by the results of series C and D, where the same materials were used with different numbers of shields. The shields substantially reduce the rate of heat transfer and the effective thermal conductivity. Increasing the number of shields would add still more to the usefulness of the insulation material; however, the weight of the insulation system would also increase.

Approved for Public Release

Contrails

Thin shield materials .0001 in. thick or less would be desirable to limit the weight increase. In future insulation systems it may be advantageous to prepare thoria fibers and space them with shielding. An alternative would be to use layers of a fine-weave graphite cloth with alternate layers of metallic shields.

An example of the benefits that can be expected from shielding is shown in Figure 18. The system considered consists of a 1-in. thick panel containing a variable number of radiation shields of negligible thickness, spaced by fibers or powder of a specific thermal conductivity. The fibers or powders are assumed to be transparent to radiation; their thermal conductivity is due to particle conduction and is independent of temperature level. The emissivity of the shields is constant at 0.4. One-dimensional heat transfer is considered. Heat transfer by conduction and radiation are considered to be additive. Additional benefits would be obtained if the powder or fiber spacers also attenuate radiation.

It is important to point out that shields cannot be used alone, since pressures lower than can be practically achieved would be required to reduce gas conduction with reasonable shield spacing. The fibrous or powdered materials reduce gas conduction and separate the shields.

Another important factor to be considered when radiation shields are used is the effect of holes for evacuation purposes. Since a hole allows radiation to pass from a hot zone to a cooler zone without attenuation or reflection, it can be considered to raise the effective emissivity of the radiation shield. For a system of perforated plane radiation shields of emissivity ε, confined by two solid plane surfaces at temperatures T_2 and T_1, the heat transfer by radiation is given as:

$$q_r = \frac{(T_2^4 - T_1^4)}{1 + (\frac{2}{\varepsilon'} - 1)\, n}$$

where n is the number of shields and ε' is the effective emissivity of the shields and is given as

$$\varepsilon' = \varepsilon + (2-\varepsilon)\,\tau$$

where τ is the fraction of the surface that is covered with holes.

Approved for Public Release

Contrails

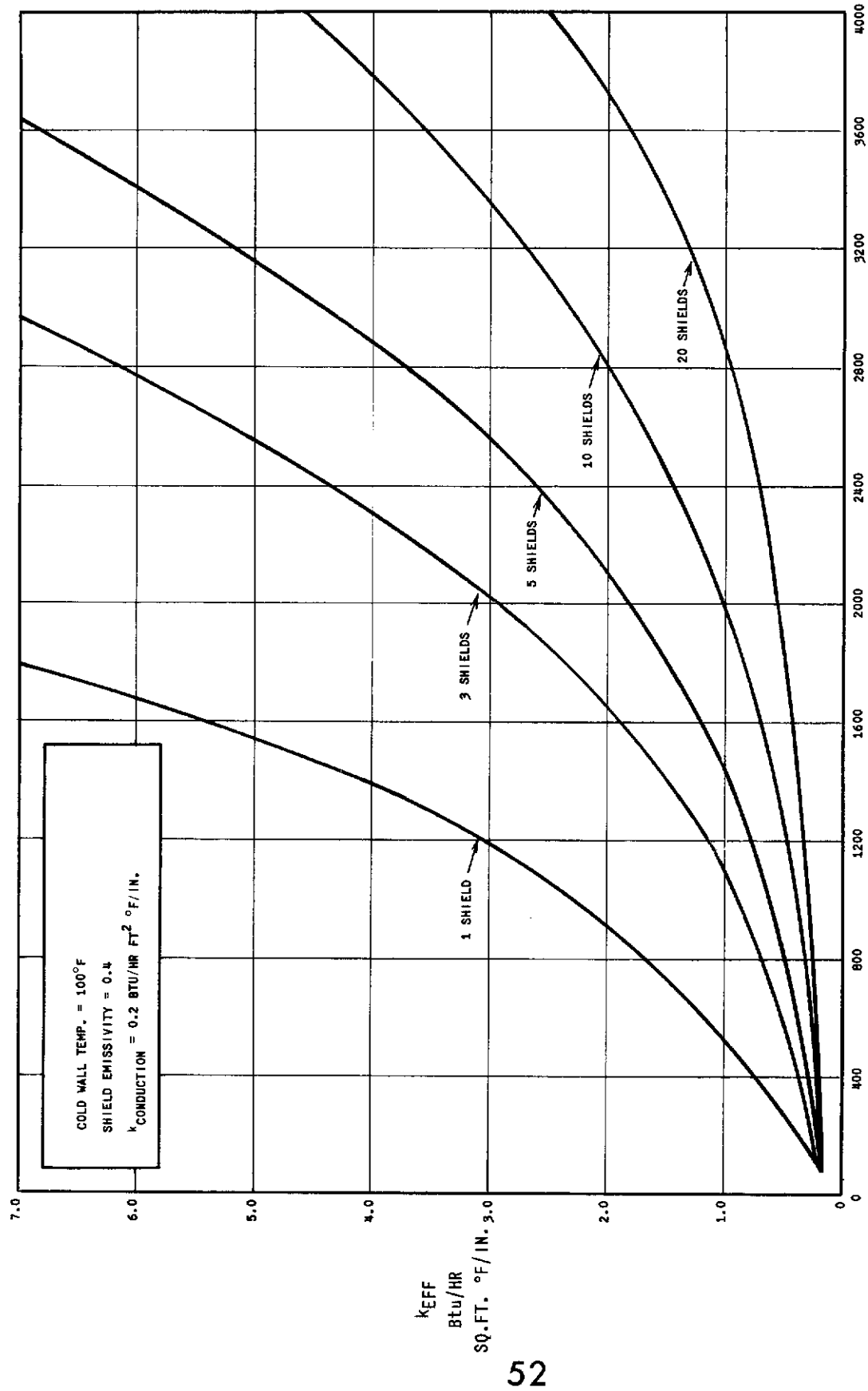

FIGURE 18 Effect of Thermal Radiation Shielding on Effective Thermal Conductivity

Approved for Public Release

Contrails

Thus, in the example mentioned previously, if 10% open area were needed for adequate evacuation of the powdered or shielded material, the effective emissivity would have increased 40%. This method of accounting for evacuation holes should be extended to take into account the absorption and scattering due to the powdered material.

In the experimental work the fraction of the shield surface that was open was less than 1%, and the increase in the effective emissivity of the shields was probably less than 5%. In insulation configurations where rapid self-evacuation is desired (for example in a re-entry vehicle), the number and size of evacuation holes becomes very important, and further investigation should give this factor due consideration.

e. Long-Term Tests

Figures 15 and 16 show that the thermal conductivity of the insulation material is not affected by long-term heating when the hot wall temperature is less than 3000°F. During the latter part of the tests of series F, thermocouples in the measuring device did not function properly, and it was impossible to obtain reliable thermal conductivity values. It was observed qualitatively that the thermal conductivity did increase with heating duration at hot wall temperatures above 3000°F. This was due to deterioration of the ADL-17, since it exceeded the maximum operating temperature. Even though thermal conductivities could not be measured, the insulation system was heated to a hot wall temperature of over 3500°F to determine if undesirable chemical reactions occurred. Observation of the materials after the tests were complete showed that at the higher temperatures, reactions of graphite-tantalum could limit the useful operating temperature of this combination for extended periods.

f. Comparison With Other Materials

Table VII compares the properties of several insulation systems considered here and several materials whose properties have been reported in the literature. The properties of the commercial materials are based upon a mean temperature and represent conditions in which the materials are not evacuated. Since gas conduction becomes smaller compared with thermal radiation as the temperature is increased, and since the hot wall temperatures greatly influence the properties of the insulation, the comparison indicated is valid. When considering the use of the insulation materials for space vehicles, the product of density and thermal conductivity is important. Values of $k_{eff} \times \rho$ for the systems investigated were substantially lower than for the other insulation materials, including zirconia and alumina foams.[18] Also, the maximum continuous operating temperatures are higher than for most available materials.

Approved for Public Release

TABLE VII

COMPARISON OF INSULATION MATERIALS

System or Material	Average Density[a] (lb/ft^3)	Thermal Conductivity (Btu/hr ft^2 °F/in.)	k_{eff} x Density	Max. Pressure for Eliminating Gas Conduction[b] (mm Hg)	Max. Continuous Operating Temperature (°F)
ADL-17	16	0.075 at 1000°F[c] 0.115 at 2000°F[c]	1.20 1.84	1	2200
ADL-17, Graphite Fibers and Tantalum Shields (0.15-in. spacing)	8.8	0.050 at 1000°F[c] 0.150 at 2000°F[c]	0.44 1.32	2×10^{-3}	2700
Graphite Fibers and Tantalum Shields (0.10-in. spacing)	9.5	0.09 at 1000°F[c] 0.24 at 2000°F[c] 0.90 at 3000°F[c]	0.86 2.38 8.60	2×10^{-3}	3500
Fibrous Potassium Titanate	3.4 12.0	0.7 at 1000°F[d] 0.52 at 1000°F[d]	2.40 6.25	Not determined	1800
Thermoflex	3.0 10.0	1.16 at 1000°F[d] 0.75 at 1000°F[d]	3.48 7.50	Not determined	2000
Refrasil	3 9	1.25 at 1000°F[d] 0.75 at 1000°F[d]	3.75 6.75	Not determined	2000

a. Density including shields of thickness 0.0005 in.
b. Based upon reducing gas conduction to .001 free gas value.
c. Based upon hot wall temperature, evacuated material.
d. Based upon mean temperature, material not evacuated.

Approved for Public Release

Contrails

IV. APPLICABILITY OF INSULATION MATERIALS

In airborne applications, both the weight of the protection system and the quantity of heat that must be rejected at a low temperature as the surface of the vehicle is heated must be considered. A complete study of the optimum shield and insulation configurations and the resultant weight and heat loads for several missions is beyond the scope of the present investigation. However, several calculations can be made to illustrate the use of the insulation systems evaluated.

Table VIII shows, for several surface temperatures and insulation systems, characteristic values of heat load, weight of insulation, etc. It is assumed that oxidation-resistant coatings will be provided for the external surface of the thermal protection system. Densities are based upon the materials used in this study, assuming that radiation shields of 0.0005 in. can be used. As an example of the coolant requirements, a water vaporization system such as "Thermosol"[19] was considered. The values presented in Table VIII should not be taken as representative of an optimum weight insulation thickness or configuration.

Approved for Public Release

TABLE VIII

CHARACTERISTICS OF THERMAL PROTECTION SYSTEMS
(Basis: 1 sq ft of Surface Area)

Insulation System	Thickness (in.)	Weight of Insulation (lb/ft^2)	Surface Temperature (°F)	Heat Rejection Load ($Btu/hr\ ft^2$)	Cooling Requirements[a] (Gallons $H_2O/hr\ ft^2$)
Graphite Fibers and Tantalum Shields	0.625	0.50	1000	130	0.016
			2000	730	0.091
			3000	4200	0.53
			4000[b]	1.12×10^4	1.40
ADL-17, Graphite Fibers and Tantalum Shields	0.625	0.46	1000	72	0.009
			2000	460	0.058
			2700	1830	0.230
ADL-17, Graphite, Thoria and Tantalum Shields	0.625	2.55	1000	61	0.008
			2000	520	0.065
			3000	3420	0.425

a. Based upon vaporization of water as the heat sink--ΔH_v = 960 Btu/lb.

b. Extrapolated to 4000°F.

Approved for Public Release

Contrails

V. CONCLUSIONS AND RECOMMENDATIONS

We conclude that thermal protection systems embodying the materials studied in combination with radiation shields act as effective thermal insulators at temperatures in excess of 3000°F over extended operating times. Although we utilized only readily available materials, their insulating performance at high temperatures points to the potential effectiveness of improved materials.

To achieve the desired improvements in high-temperature thermal protection systems we recommend that future work be carried out in the following areas: materials research, insulation system development, and measuring techniques.

A. MATERIALS RESEARCH

At the high temperatures encountered in these tests, the insulation components reacted to a greater extent than could be predicted by preliminary work. If tantalum foil of thin gauge is to be used as an insulation component, the reaction between tantalum and graphite should be investigated more thoroughly to determine if surface treatment of the tantalum or graphite could reduce the reaction rate. The high-temperature reactions between other refractory metals and graphite should also be investigated. Since thoria appeared to be inert to both tantalum and graphite at temperatures above 3000°F, methods for reducing the density and degree of compaction should be investigated. A good solution would be the preparation of thoria fibers resulting in a decreased density and less chance of sintering. Pending an investigation of the high-temperature reactivity of carbon and thoria, it may be possible to combine the materials to have a composite fiber mat that will attenuate radiation more rapidly than thoria fibers alone. The use of carbon fibers that have not been graphitized as an insulation component also warrants investigation.

Great benefit could be gained from a knowledge of the optical properties of the materials, their absorption and scattering cross sections, and the effect of density, temperature, and material additives on these properties. It would then be possible to estimate the heat-transfer properties of the materials without resorting to lengthy thermal conductivity tests. Further thermal conductivity tests of the most interesting materials are still necessary to confirm the predicted performance.

Approved for Public Release

Contrails

B. INSULATION CONFIGURATION DEVELOPMENT

Our tests indicate that radiation shielding is a prime requisite of insulation systems. Several configurations of materials can be envisioned--thin shields spaced by thin fiber layers for example. It would be desirable to test several fiber thicknesses as well as the several types of graphite fibers that are currently available. The influence of evacuation holes must be considered more thoroughly. Of particular importance is the rate of evacuation of the fibrous insulation material, which would be governed by the size holes and the temperature and pressure environment of the insulation system. Fundamental investigations of the rate of outgassing and the mechanism of transport of gases through insulation materials and shields would greatly aid design procedures for actual insulation systems.

In order to extend thermal conductivity data to other configurations and dimensions, thermal conductivity tests should be carried out over a range of insulation thicknesses and temperatures. This will determine if the thermal conductivity of a multi-component insulation system including radiation shields is a function of temperature only and not affected by geometry. Such data are important when it is necessary to optimize weight loads associated with insulation materials and coolants.

Studies should be conducted to determine other methods of heat rejection from the cold wall of a thermal protection system. The use of endothermic, homogeneous, or catalytic gas reactions for cooling mechanisms gives the advantages of high effective heat capacity and low density.

C. MEASURING TECHNIQUES

Several ways of improving the techniques of thermal conductivity measurement were suggested in the present work. The design of the thermal conductivity apparatus can be changed to provide for more uniform cooling of the measuring section and greater reliability over a larger range of heat flux. This will enable more reliable measurement of thermal conductivities at hot wall temperatures near 4000°F. Further work is indicated on the measurement of both temperature and pressure within the insulation materials. Fortunately, most insulation materials are nonconductive, and thermocouple insulation could be fabricated of the test material itself. The use of high-temperature thermocouples is not as well developed as desired. Materials other than tungsten-rhenium should be investigated. Pressure measurement within an insulation material is complex and difficult, and it warrants specific attention.

Approved for Public Release

Contrails

VI. APPENDIXES

Approved for Public Release

Contrails

APPENDIX A

SOLID CONDUCTION IN POWDERED MATERIALS

In this appendix an equation for the effective thermal conductivity for heat transfer by solid conduction is derived for a material consisting of small elastic spheres. The spheres are arranged in a simple geometric pattern corresponding to the most open packing (spheres arranged in columns and rows). We have assumed that the material is under a moderate load, which is the same in all directions. It is also assumed that any gaseous films adsorbed on the particles are small and will have a negligible effect on the mechanism of heat transfer.

From the theory of elasticity, it is known that the radius of contact "a" for two elastic spheres of radii R_1 and R_2 under a load "P" is given as:[26]

$$a = \sqrt[3]{\frac{3\ \pi P\ (K_1 + K_2)\ R_1\ R_2}{4\ (R_1 + R_2)}} \qquad (1)$$

where: $K_i = \dfrac{1 - \nu_i^2}{\pi E_i}$ $\qquad i = 1, 2$

and: E = modulus of elasticity

ν = Poisson's ratio

For equal-diameter spheres, equation 1 reduces to:

$$a = \sqrt[3]{\frac{3\ P(1 - \nu^2)\ R}{4 \quad E}} \qquad (2)$$

If we consider the x direction as lying along one of the rows or columns of spheres, and if we consider only the gradients in the x direction (see sketch below) we may write an expression for heat flow in this direction as follows:

Approved for Public Release

Contrails

$$\pi K y^2 T'' \delta x + \pi 2 K y T' \delta y = 0 \qquad (3)$$

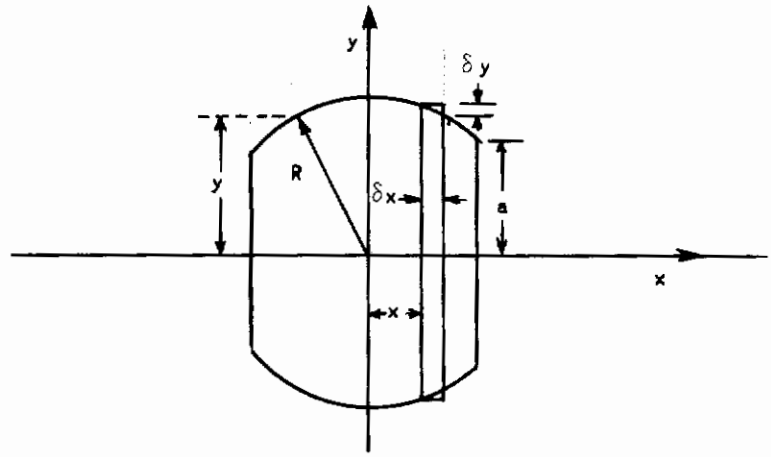

where T is the temperature and the primes denote differentiation with respect to x.

Noting that: $x^2 + y^2 = R^2$

and that: $y' = -\frac{x}{y}$

we have: $(R^2 - x^2) T'' - 2xT' = 0 \qquad (4)$

which has the solution:

$$C_1 T + C_2 = R^2 x - \frac{x^3}{3} \qquad (5)$$

where C_1 and C_2 are arbitrary constants. Noting that when $y = a$

$$x = \pm \sqrt{R^2 - a^2}$$

and using the conditions:

$$x = -\sqrt{R^2 - a^2} \qquad T = T_1$$

$$x = +\sqrt{R^2 - a^2} \qquad T = T_2$$

Approved for Public Release

Contrails

we have:

$$C_2 = \frac{C_1 (T_1 + T_2)}{2} \tag{6}$$

and

$$C_1 = \frac{1}{T_1 - T_2} \left[\frac{2}{3} (R^2 - a^2)^{3/2} - 2R^2 (R^2 - a^2) \right]^{1/2} \tag{6a}$$

Differentiating (5) with respect to x and substituting in (6a) for C_1 we have:

$$\frac{dT}{dx} = - \frac{3 (R^2 - x^2) (T_1 - T_2)}{2 (R^2 - a^2)^{1/2} (2 R^2 + a^2)} \tag{7}$$

The heat flow in the x direction for one sphere is given by:

$$Q_{ix} = k \pi a^2 \frac{dT}{dx} \Bigg|_{x = \sqrt{R^2 - a^2}} \tag{8}$$

where k is the thermal conductivity of the material. From (7) we have:

$$Q_{ix} = - \frac{3 k \pi a^4 (T_1 - T_2)}{2 (R^2 - a^2)^{1/2} (2R^2 + a^2)} \tag{9}$$

We may write an expression for the heat flow through a row of n spheres by noting that:

$$Q_{Ox} = Q_{1x} = Q_{2x} = \ldots\ldots Q_{nx}$$

and using (9) we get:

$$Q_x = - \frac{3 k \pi a^4 (T_{ox} - T_{nx})}{2 n_x (R^2 - a^2)^{1/2} (2R^2 + a^2)} \tag{10}$$

Approved for Public Release

Contrails

If there are n_x spheres per unit length and $n_y \times n_z$ spheres per unit cross section, the heat flux per unit area is given by:

$$q_x = - \frac{3\pi k n_y n_z a^4}{2 n_x (R^2 - a^2)^{1/2} (2R^2 + a^2)} \frac{\Delta T}{\Delta x} \tag{11}$$

Remembering that the load is the same in all directions we may write similar expressions for the heat flow in the y and z directions by interchanging the x, y, and z's in equation (11).

Noting that:

$$n_x = n_y = n_z = \frac{1}{2\sqrt{R^2 - a^2}}$$

we may write equation (11) as:

$$q_x = - \frac{3 \pi k a^4}{4 (R^2 - a^2) (2R^2 + a^2)} \tag{12}$$

If $a \ll R$ we have:

$$q_x \approx - \frac{3 \pi k a^4}{8 R^4} \cdot \frac{\Delta T}{\Delta x} \tag{13}$$

remembering that the heat flow is one dimensional and that:

$$\vec{q} = i q_x + j q_y + K q_z \tag{14}$$

we have from (13) and (14):

$$\vec{q} \approx - \frac{3 \pi k a^4}{8 R^4} \left[i \frac{\Delta T}{\Delta x} + j \frac{\Delta T}{\Delta y} + K \frac{\Delta T}{\Delta z} \right] \tag{15}$$

and if there are a large number of small spheres in a unit length we have:

$$\vec{q} \approx - \frac{3 \pi k a^4}{8 R^4} \nabla T \tag{16}$$

Approved for Public Release

Contrails

If we define k_{eff} as:

$$\frac{\bar{q}}{\nabla T} = - k_{eff} \tag{17}$$

we have:

$$k_{eff} = \frac{3\pi k a^4}{8 R^4} \tag{18}$$

The load per unit area F is given by:

$$F = P n^2 \tag{19}$$

or for $a \ll R$:

$$F \tilde{\approx} \frac{P}{4 R^2} \tag{20}$$

substituting (20) into (2) and (2) into (18) we get finally:

$$k_{eff} = \frac{3 \pi k}{8} \left[\frac{3}{E} (1 - \nu^2) F \right]^{4/3} \tag{21}$$

Approved for Public Release

Contrails

APPENDIX B

ANALYSIS OF GAS CONDUCTIVITY AND EFFECTS OF PARTICLE SIZE AND PRESSURE

From the Kinetic Theory of gases[20] the thermal conductivity of a gas at low density is given by

$$k = N\rho\ c_v\ \bar{v}\ L \tag{1}$$

provided the accommodation coefficient is unity.

The accommodation coefficient[23] takes into account that at low pressures the transfer of heat by the gas is no longer the result of a diffusion along a random path, and that a sharp temperature discontinuity may exist at the surface of each particle. Possible values of the accommodation coefficient lie between 0 (corresponding to no thermal interaction between the particle and an impinging molecule) and 1 (corresponding to complete thermal equilibrium). In practice this coefficient varies with the gas, the nature of the surface, and the temperature[24], and as a result it has to be evaluated for the particular material to be studied.

Over a wide range of pressures thermal conductivity of a gas is independent of pressure because the mean free path of the gas varies directly with the pressure. When the pressure is reduced below the point where the mean free path of the gas is less than the distance between the walls or particles against which molecules strike, thermal conductivity becomes proportional to the pressure. At these pressures the mean free path length of the molecules, taking into account both collisions between gas molecules and between gas molecules and a surface, becomes:

$$L = Lg\ \frac{d}{d+Lg} \tag{2}$$

where d is the average distance a gas molecule can travel in the direction of heat flow before collision with a solid barrier.

It has been shown that the mean molecular velocity is proportional to the square root of the temperature:

$$\bar{v}\ \alpha\sqrt{T} \tag{2a}$$

that the specific heat is a function of temperature:

$$c_v = f\,(T) \tag{2b}$$

---

* See Nomenclature for Appendix A at end of this appendix.

Approved for Public Release

Contrails

and that the mean free path of a gas is inversely proportional to the pressure:

$$Lg \propto \frac{1}{P} \tag{2c}$$

Hence:

$$\rho Lg \propto \frac{\rho}{P} \propto \frac{1}{T} \tag{2d}$$

Combining equation 1 and 2 thermal conductivity can be written as:

$$k = A(T)\frac{d}{d + Lg} \tag{3}$$

Writing equation 3 for temperature conditions $T = T_o$ and combining with equation (2c) we have:

$$k_{PT_o} = A(T_o) \frac{d}{d + \frac{P_o}{P} Lg_o} \tag{4}$$

where

$$Lg_o = Lg \text{ at } P_o \text{ and } T_o$$

Letting d be much larger than Lg and letting P be at atmospheric pressure, then:

$$k_{P_o T_o} = A(T_o) \tag{5}$$

which is the normal gas conductivity at P_o and T_o.

Letting,

$$\alpha_{T_o} = \left(\frac{k_P}{k_{P_o}} \right)_{T_o}$$

then on substituting equation 5 in equation 4,

$$\alpha_{T_o} = \frac{\bar{x}}{1 + \bar{x}} \tag{6}$$

where,

$$\bar{x} = \frac{Pd}{L_{g_o} P_o} \tag{7}$$

Approved for Public Release

Contrails

Solving equation 6 for $\bar{x}$ we have

$$\bar{x} = \frac{\alpha_{T_o}}{1 - \alpha_{T_o}} \qquad (8)$$

Also from Kinetic Theory it can be shown that at constant pressure

$$Lg \ \alpha \ T^{n+\frac{1}{2}} \qquad (20) \qquad (9)$$

Using equation 9 we can write equations 7 and 8 for any temperature T as:

$$\bar{x} = \frac{Pd}{P_o Lg_o} \left(\frac{T_o}{T} \right)^{n+\frac{1}{2}} \qquad (10)$$

$$\bar{x} = \frac{\alpha_T}{1 - \alpha_T} \qquad (11)$$

where

$$\alpha_T = \left(\frac{k_P}{k_{P_o}} \right)_T$$

Therefore given the mean distance equations 10 and 11 can be used to evaluate gas conductivity.

The mean distance d can be evaluated in terms of the physical properties of the medium using one of the following approaches:

(a) Geometrical Approximation

Consider the solid part of the insulating powder made up of uniform spheres packed in a geometric lattice. For the closest packing[25] the volume of a void space is given by

$$V_v = 0.18 \, D^3$$

Approved for Public Release

Contrails

For the most open packing the volume of a void space is given by:

$$V_v = 0.48\, D^3$$

Assuming that the volume of the void space is spherical,

$$V_v = \frac{4}{3}\pi\, d^3$$

where d is the mean distance between adjacent particles.

Therefore for the closest packing,

$$d = 0.351\, D$$

for the most open packing,

$$d = 0.486\, D$$

and for an intermediate packing,

$$d = 0.418\, D$$

(b) Empirical Shape Factor

Let us introduce a shape factor S which has to be determined experimentally for a given insulating powder. For a large number of irregularly shaped spaces it can be shown that the statistical distribution of the characteristic dimension of this space is proportional to the average volume of a space, provided such a dimension is measured consistently from space to space. This assumption would not hold if there were large voids unevenly distributed through the insulating powder.

Therefore, if we let d be the characteristic mean distance we have:

$$d^3 \propto V_v \tag{12}$$

If the number of voids equals the number of particles in a unit volume:

$$V_v = \frac{\phi}{N} \tag{13}$$

Approved for Public Release

Contrails

The average volume occupied by a single particle is given by (25)

$$\frac{1}{N} = \frac{a_v D^3}{1 - \phi} \tag{14}$$

where a_v is the volume shape-factor.

Although voids have to be determined experimentally except for ideal arrangements of spheres, the voids can be represented in terms of the true and apparent density by:

$$\phi = (1 - \frac{\rho_a}{\rho}) \tag{15}$$

Combining equations 12 through 15 we have:

$$d \propto \left(\frac{\rho}{\rho_a} - 1\right)^{1/3} D \tag{16}$$

Defining the shape factor S as the constant of proportionality in equation 16 we have:

$$d = S \left(\frac{\rho}{\rho_a} 1\right)^{1/3} D$$

In order to make use of this more accurate expression the shape factor would have to be experimentally evaluated for each material.

The mean distance based on the geometrical approximation was used to evaluate the relationship between particle diameter and gas pressures for various fractions of the atmospheric gas conductivity as Figure 9 shows.

It is of interest to note that at higher temperatures the mean free path is longer. Therefore, higher pressures will give the same gas conductivity for a specific particle diameter as compared to the pressures required at lower temperatures.

Approved for Public Release

Contrails

NOMENCLATURE FOR APPENDIX B

k	Thermal conductivity
N	Constant number of particles per unit volume
ρ	Density
c_v	Specific heat at constant volume
$\bar{v}$	Mean molecular speed
L	Effective mean free path length
L_g	Mean free path length between gas molecules
d	Average distance a gas molecule can travel in the direction of heat flow before collision with a solid barrier
T	Absolute temperature
P	Pressure
A	A(T) a function of the absolute temperature
α	k_P/k_{P_o}
$\bar{x}$	$\frac{Pd}{L_{g_o}P_o}$
n	Constant
V	Volume
D	Mean particle diameter
ϕ	Fraction of space occupied by voids
a_v	Volume shape factor

Approved for Public Release

Contrails

NOMENCLATURE (Continued)

Subscripts

o	Reference conditions
v	Void space
T	At temperature T
P	At pressure P
∞	P_o T_o for P_o = Atmospheric pressure

Approved for Public Release

Contrails

APPENDIX C

RADIANT HEAT TRANSFER THROUGH POWDERED INSULATION

In the following discussion we will consider the steady heat flow through an infinite powdered insulation in the form of a plate of sufficient thickness to be considered homogenous[21,22]. We will assume that radiations can be propagated in two directions only, forward and backward along the x axis. Let the vector i_2 designate the monochromatic radiant flux in the positive x direction and the vector i_1 designate the flux in the reverse direction. A monochromatic flux is defined as the amount of radiant power between wave lengths λ and $\lambda + d\lambda$ passing through a unit area normal to the direction of propagation.

The mechanisms causing change in the rate of radiant transfer are absorption, reradiation, and scattering.

In general, the scattering process which occurs in porous materials is extremely complicated. Therefore we will assume that the scattered radiation can be resolved into a forward component and a backward component. We will let F be the fraction of the scattered radiant energy which continues to travel in the forward direction of the incident beam and B the component which is reflected backward.

Therefore:

$$F + B = 1 \qquad (1)$$

We will now introduce the scattering cross section S_S. S_S is defined as the fraction of the radiant energy scattered from a beam carrying one unit of energy per unit area normal to the direction of propagation. The probability that a photon will be scattered in the distance dx is proportional to $n\, S_S\, dx$, where n is the number of scattering particles per unit volume of the material.

In order to consider the absorption process we will introduce the absorption cross section S_a defined as the fraction of the power absorbed from a beam carrying one unit of energy per unit area normal to the direction of propagation.

The total rate of absorption by a body in equilibrium must equal the total rate of emission.

Approved for Public Release

Contrails

We may now proceed to describe how the various radiation mechanisms affect the radiant heat transfer rate through the material. Let us examine the change in each flux vector as it passes through a small volume of insulation. The faces of this volume are one unit in area parallel to the boundaries of the insulation and perpendicular to the x axis. The change in the flux vector i_2 in traveling from x to $x + \Delta x$ is given by:

$$\Delta i_2 = -n (S_{s_\lambda} + S_{a_\lambda}) i_2 \Delta x + n F_\lambda S_{s_\lambda} i_2 \Delta x$$

$$+ n B_\lambda S_s \; i \Delta x + n \varepsilon_\lambda A g(\lambda, T) \; \Delta x \qquad (2)$$

where n is the number of bodies scattering energy per unit volume, $S_{s\lambda}$ is the monochromatic scattering cross section per scattering body in the insulation, $S_{a\lambda}$ is the monochromatic absorption cross section per scattering body in the insulation, Δx is the volume of the insulation, A is the emitting area per body in the insulation, and ε_λ is the emissivity of the insulation.

The function $g(\lambda, T)$ is Planck's radiation function which gives the energy radiated at each wave length for a black body. Dividing equation 2 by Δx and taking the limit as $\Delta x \to 0$ we have:

$$\frac{d_{i_2}}{dx} = -n (S_{s_\lambda} + S_{a_\lambda}) i_2 + n F_\lambda S_{s_\lambda} i_2$$

$$+ n B_\lambda S_{s_\lambda} i_1 + n \varepsilon_\lambda A g(\lambda, T) \qquad (3)$$

Substituting equation 1 into equation 3 we have:

$$\frac{d_{i_2}}{dx} = -n (B_\lambda S_{s_\lambda} + S_{a_\lambda}) i_2 + n B_\lambda S_{s_\lambda} i_1$$

$$+ n \varepsilon_\lambda A g(\lambda, T) \qquad (4)$$

Approved for Public Release

Contrails

If we now assume that the radiation is continuous over the spectrum and contains all wave lengths we may introduce the spectrally integrated flux I defined as:

$$I = \int_0^\infty i(\lambda)\, d\lambda \tag{5}$$

Introducing equation 5 into equation 4 we have:

$$\frac{dI_2}{dx} = -n(BS_S + S_a) I_2 + n BS_S I_1 + n \varepsilon A \sigma T^4 \tag{6}$$

where σT^4 is the integral of Planck's function:

$$\sigma T^4 = \int_0^\infty g(\lambda, T)\, d\lambda = \int_0^\infty \frac{c_1 \lambda^{-5} d\lambda}{\varepsilon^{c_2/\lambda T} - 1} \tag{7}$$

where σ is the Stefan-Boltzmann constant, and T is the absolute temperature, and where c_1 and c_2 are Planck's radiation constants.

The values B, S_S, S_a and ε are average values over the spectrum so that:

$$BS_S = \frac{1}{I_2} \int_0^\infty BS_{S_\lambda}\, i_2\, d\lambda \tag{8a}$$

$$S_a = \frac{1}{I_2} \int_0^\infty S_{a_\lambda}\, i_2\, d\lambda \tag{8b}$$

$$\varepsilon = \frac{1}{\sigma T^4} \int_0^\infty \varepsilon_\lambda\, g(\lambda, T)\, d\lambda \tag{8c}$$

If we now assume that the gas is completely transparent to radiation and the solid particles are partially transparent or opaque, Kirchhoff's law applies for any temperature T:

$$J^2 S_a(T) = \varepsilon(T) A \tag{9}$$

where J is the index of refraction of the solid.

Approved for Public Release

Contrails

Equation 6 now becomes:

$$\frac{dI_2}{dx} = -n(BS_S + S_a) I_2 + n BS_S I_1$$

$$+n J^2 S_a \sigma T^4 \qquad (10)$$

For convenience let:

$$N = n BS_S$$

$$P = n S_a \qquad (11)$$

where N is the scattering cross section, and P is the absorption cross section. Using these parameters in equation 10 gives:

$$\frac{dI_2}{dx} = -(N + P) I_2 + N I_1 + P J^2 \sigma T^4 \qquad (12)$$

In a completely analogous manner we may write an expression for the other flux component I_1 :

$$-\frac{dI_1}{dx} = -(N + P) I_1 + N I_2 + P J^2 \sigma T^4 \qquad (13)$$

If we assume that the void spaces are too small for convection to occur we have from the continuity equation:

$$q_T = q_c + q_r \qquad (14)$$

where q_c is the heat flux due to conduction, q_r is the heat flux due to radiation and q_T is the total heat flux. From Fourier's equation:

$$q_c = -k_c \frac{dT}{dx} \qquad (15)$$

where k_c is the effective thermal conductivity of the material.

Approved for Public Release

Contrails

The radiant heat flux must be given by:

$$q_r = I_2 - I_1 \tag{16}$$

and equation 14 becomes:

$$q_T = -k_c \frac{dT}{dx} + I_2 - I_1 \tag{17}$$

Differentiating equation 17 with respect to x we have:

$$\frac{dq_T}{dx} = -k_c \frac{d^2 T}{dx^2} + \frac{dI_2}{dx} - \frac{dI_1}{dx} = O \tag{18}$$

Provided k_c is constant, substitution of equations 12 and 13 into 18 gives:

$$-k_c \frac{d^2 T}{dx^2} - P(I_2 + I_1) + 2PJ^2 \sigma T^4 = O \tag{19}$$

Subtracting equation 13 from equation 12 we have:

$$\frac{d}{dx}(I_2 + I_1) = -(P+2N)(I_2 - I_1) \tag{20}$$

Substitution of equations 17 and 19 into equation 20 gives:

$$\frac{d}{dx}\left(\frac{2PJ^2 \sigma T^4 - k_c \frac{d^2 T}{dx^2}}{P}\right)$$

$$= -(P + 2N)\left(k_c \frac{dT}{dx} + q_T\right) \tag{21}$$

Approved for Public Release

Contrails

Upon integration we obtain:

$$2J^2 \sigma T^4 - \left(\frac{k_c}{P}\right)\left(\frac{d^2T}{dx^2}\right)$$

$$= - k_c (P + 2N) T - [(P + 2N) q_T] x + C \qquad (22)$$

where C is a constant of integration.

Combining equations 17 and 19 with equation 22 we obtain:

$$2 I_2 = - k_c (P + 2 N) T - [(P + 2 N) q_T] x$$

$$+ C + q_T + k_c \frac{dT}{dx} \qquad (23)$$

$$2 I_1 = - k_c (P + 2N) T - [(P + 2N) q_T] x$$

$$+ C - q_T - k_c \frac{dT}{dx} \qquad (24)$$

If the powdered insulation is between two surfaces with the same emissivity (ε_o) at x = 0 and x = L then we have the boundary conditions:

$$x = O, T = T_o \qquad I_2 (O) = J^2 \varepsilon_o \sigma T_o^4 + (1 - \varepsilon_o) I_1 (O) \qquad (25a)$$

$$x = L, T = T_L \qquad I_1 (L) = J^2 \varepsilon_o \sigma T_L^4 + (1 - \varepsilon_o) I_2 (L) \qquad (25b)$$

If we consider radiation as being more important than conduction as a mechanism for heat transfer, we may set k_c equal to zero.

Approved for Public Release

Contrails

Equations 23 and 24 now become:

$$2 I_2 = - [(P + 2N) q_T] x + C + q_T \tag{23a}$$

$$2 I_1 = - [(P + 2N) q_T] x + C - q_T \tag{24a}$$

and equation 22 becomes:

$$T^4 = \frac{C}{2J^2 \sigma} - \left[\frac{(P + 2N) q_T}{2 J^2 \sigma} \right] x \tag{22a}$$

Substituting the conditions 25a and 25b into equations 23 and 24 and solving for q_T and C we have:

$$q_T = \frac{2J^2 \sigma (T_o^4 - T_L^4) \varepsilon_o}{[\varepsilon_o (P + 2 N) L + 4 - \varepsilon_o]} \tag{26}$$

where,

$$C = 2 J^2 \sigma \frac{(T_o^4 + T_L^4)}{2} + \frac{2 J^2 \sigma (P + 2N) L \varepsilon_o (T_o^4 - T_L^4)}{2 [4 - 2 \varepsilon_o + \varepsilon_o (P + 2N) L]} \tag{27}$$

Substituting equations 26 and 27 into 22a we have:

$$T^4 = \frac{T_o^4 + T_L^4}{2} + \left[\frac{\varepsilon_o (P + 2N) (T_o^4 - T_L^4)}{4 - 2 \varepsilon_o + \varepsilon_o (P + 2N) L} \right] \left(\frac{L}{2} - x \right) \tag{28}$$

Equation 28 indicates that T^4 is a function of distance depending upon the radiation characteristics of the particular material, and that for $x = L/2$, T^4 is given by the arithmetic mean of the fourth power of the boundary temperatures.

Approved for Public Release

Contrails

REFERENCES

1. Kubaschewski, D., and Evans, E. L., Metallurgical Thermochemistry, Permagon Press, Ltd., New York (1958)

2. Quill, L., Chemistry and Metallurgy of Miscellaneous Materials, McGraw-Hill Book Company, Inc., New York (1950)

3. Hodgman, C. D., ed., Handbook of Chemistry and Physics, 40th Edition, Chemical Rubber Publishing Company, Cleveland (1958)

4. Chemical and Engineering News, p. 41, April 14, 1958

4a. Battelle Memorial Institute, DMIC Memo 67, September 20, 1960

5. Johnson, P. D., Journ. Amer. Ceramic Soc., 33, 168 (1950)

6. MacKenzie, J. K., and Shuttleworth, R., Proc. Phys. Soc., B62, 833 (1949)

7. Weyl, W. A., Ceramic Age, 60, 28 (1952)

8. Kingery, W. D., and Berg, M., Journ. Appl. Phys., 26, 1205 (1955)

9. Kuczynski, G. C., Acta Met, 4, 58 (1956)

10. Mapother, D., Crooks, H. N., and Mauren, R., Journ. Chem. Phys., 18, 1231 (1950)

11. Schmidt, F. F., Tantalum and Tantalum Alloys, DMIC Report 133, Battelle Memorial Institute, Contract AF18(600)-1375, p. 169-170 (1960)

12. Strong, H. M., Bundy, F. P., and Bovenkerk, H. P., Journ. Appl. Phys., 31, p. 39 (1960)

13. Verschoor, J. D., and Greebler, P., Trans. ASME, August, 1952, p. 961

14. MacAdams, W. H., Heat Transmission, p. 290, Third Edition, McGraw-Hill Book Company, New York (1954)

Approved for Public Release

Contrails

15. Schotte, W., "Thermal Conductivity of Insulating Powders," AlChE JOURNAL, 6, 63 (1960)

16. Gubareff, G. G., Shao-Yen Ko, McNall, P. E., "Review of Thermal Radiation Property Values for Metals and Other Materials," Minneapolis-Honeywell Regulator Co., Hopkins, Minn. (1958)

17. Hottel, H. C., in Heat Transmission by MacAdams, W. H., Third Edition, McGraw-Hill Book Co., New York (1954)

18. Quarterly Progress Reports, The Martin Company under Contract AF33(616)-7497, Project 1368, Task 13719

19. Alvis, J. F., and Whisenhunt, G. B., A Thermal Protection System for Lifting Re-entry Vehicles - Presented at ARS Lifting Re-entry Vehicles: Structures, Materials and Design Conference, April 6, 1961

20. Kennard, E. H., Kinetic Theory of Gases, McGraw-Hill Book Company, Inc., New York (1938)

21. Larkin, B. K., Unpublished Thesis, University of Michigan (1957)

22. Hamaker, H. C., Philip Research Reports,2, 55, 103 (1947)

23. M. Knudsen, Ann Physik,34, 593 (1911)

24. Bremner, J.G.M., Proc. Roy. Soc. 201A, 305 (1950)

25. Dalla Valle, J. M., MicroMeritics, 103, 110, Pitman Publishing Corp., New York (1943)

26. Timoshenko, S., and Goodier, J. N., Theory of Elasticity, McGraw-Hill Book Company, Inc., New York (1951)

Approved for Public Release